NISTIR 7454

Effect of CuO Nanolubricant on R134a Pool Boiling Heat Transfer with Extensive Measurement and Analysis Details

Mark A. Kedzierski
Maoqiong Gong

National Institute of Standards and Technology
Technology Administration, U.S. Department of Commerce

NISTIR 7454

Effect of CuO Nanolubricant on R134a Pool Boiling Heat Transfer with Extensive Measurement and Analysis Details

Mark A. Kedzierski

U.S DEPARTMENT OF COMMERCE
National Institute of Standard and Technology
Building Environment Division
Building and Fire Research Laboratory
Gaithersburg, MD 20899-8631

Maoqiong Gong

Chinese Academy of Sciences
Beijing, China

September 2007

U.S. Department of Commerce
Carlos M. Gutierrez, Secretary

National Institute of Standards and Technology
James M. Turner, Acting Director

Effect of CuO Nanolubricant on R134a Pool Boiling Heat Transfer with Extensive Measurement and Analysis Details

M. A. Kedzierski
National Institute of Standards and Technology
Bldg. 226, Rm B114
Gaithersburg, MD 20899
Phone: (301) 975-5282
Fax: (301) 975-8973

M. Gong
Chinese Academy of Sciences
Beijing, China

ABSTRACT
This paper quantifies the influence of CuO nanoparticles on the boiling performance of R134a/polyolester mixtures on a roughened, horizontal, flat surface. Nanofluids are liquids that contain dispersed nano-size particles. A lubricant based nanofluid (nanolubricant) was made with a synthetic ester and 30 nm diameter CuO particles stably suspended in the mixture to a 4 % volume fraction. For the 0.5 % nanolubricant mass fraction, the nanoparticles caused a heat transfer enhancement relative to the heat transfer of pure R134a/polyolester (99.5/0.5) of between 50 % and 275 %. A smaller enhancement was observed for the R134a/nanolubricant (99/1) mixture, which had a heat flux that was on average 19 % larger than that of the R134a/polyolester (99/1) mixture. Further increase in the nanolubricant mass fraction to 2 % resulted in a still smaller boiling heat transfer improvement of approximately 12 % on average. Consequently, significant refrigerant/lubricant boiling heat transfer enhancements are possible with nanoparticles. Thermal conductivity measurements and a refrigerant\lubricant mixture pool-boiling model were used to suggest that increased thermal conductivity is responsible for only a small portion of the heat transfer enhancement due to nanoparticles. Further research with nanolubricants and refrigerants are required to establish a fundamental understanding of the mechanisms that control nanofluid heat transfer.

Keywords: additives, boiling, copper (II) oxide, enhanced heat transfer, nanotechnology, refrigerants, refrigerant/lubricant mixtures

TABLE OF CONTENTS

LIST OF FIGURES

LIST OF TABLES

INTRODUCTION

The U.S. National Nanotechnology Initiative (NNI) has supported an explosion of research in recent years including the investigation of the heat transfer properties of liquids with dispersed nano-size particles called nanofluids. Prior to the initiative, nanofluids research was mainly confined to thermal conductivity investigations. Eastman et al. (2001) found that the thermal conductivity of some nanofluids, with nanoparticles at a volume fraction of less than 0.4 % results in the nanofluid having a thermal conductivity that was more than 40 % greater than that of the pure base fluid. Herein lies what is believed to be a great potential for the enhancement of liquid heat transfer by the addition of nanoparticles to the base fluid.

Water, ethylene glycol, and lubricants have been successfully used as base fluids in making stable nanofluids where the particles remain suspended in the liquid. Although water based nanofluids are the least stable of the three liquids because of the relatively low viscosity of water, most of the boiling heat transfer studies have been conducted with water based nanofluids (Bang and Chang (2004), Wen and Ding (2005), and You et al. (2003)). Although, You et al. (2003) and Bang and Chang (2004) did not observe a pool-boiling enhancement with nanofluids, Wen and Ding (2005) did. Consequently, there is a potential for boiling heat transfer improvement with nanofluids even though the mechanisms that govern the improvement are not fully understood.

Currently, there are no published measurements to determine if nanoparticles can improve refrigerant/lubricant boiling heat transfer. One reason for this might be that although the nanoparticles are expected to form a stable suspension with the lubricant, once the nanolubricant is mixed with the refrigerant the nanoparticles will become unstable with respect to the refrigerant/lubricant mixture because the relatively low viscosity of the mixture discourages Brownian motion. This potential outcome, however, may not prohibit the application of nanoparticles to air-conditioning equipment because the mechanism of the boiling heat transfer of refrigerant/lubricant mixtures is strongly governed by the lubricant excess layer that resides at the boiling surface (Kedzierski, 2003a). There is reason to believe that the boiling will drive the nanoparticles to the heat transfer surface where they will become stable and remain within the lubricant excess layer. Some of the particles will also be entrained in the vigorous boiling of the fluid. If the nanoparticles significantly change the thermal conductivity of the lubricant excess layer, that may cause an enhancement or a degradation in heat transfer depending on whether the increased conduction causes a reduced available superheat or whether it increases the thermal boundary layer thickness. The potential for a boiling heat transfer enhancement is likely to depend on the material of the particles, their shape, size, distribution, and concentration.

In order to investigate the influence of nanoparticles on refrigerant/lubricant pool boiling, the boiling heat transfer of three R134a/nanolubricant mixtures on a roughened, horizontal, flat (plain), copper surface was measured. A commercial polyolester lubricant (RL68H[1]) with a nominal kinematic viscosity of 72.3 $\mu m^2/s$ at 313.15 K was the base lubricant that was mixed

[1] Certain commercial equipment, instruments, or materials are identified in this paper in order to specify the experimental procedure adequately. Such identification is not intended to imply recommendation or endorsement by the National Institute of Standards and Technology, nor is it intended to imply that the materials or equipment identified are necessarily the best available for the purpose.

with nominally 30 nm diameter copper (II) oxide (CuO) nanoparticles. Copper (II) oxide (79.55 g/mol) has many commercial applications including use as an optical glass-polishing agent. A manufacturer used a proprietary surfactant at a mass between 5 % and 15 % of the mass of the CuO as a dispersant for the RL68H/CuO mixture (nanolubricant). The manufacturer made the mixture such that 40 % of the volume was CuO particles. The mixture was diluted in-house to a 4 % volume fraction of CuO by adding neat RL68H (see Appendix C) and ultrasonically mixing the solution for approximately 24 h. The particle size and dispersion were verified by a light scattering technique and was found to be approximately 35 nm and well dispersed with little particle agglomeration (Sung, 2006). The RL68H/CuO (96/4)[2] volume fraction mixture, a.k.a. RL68H4Cu, was mixed with pure R134a to obtain three R134a/RL68H4Cu mixtures at nominally 0.5 %, 1 %, and 2 % mass fractions for the boiling tests. In addition, the boiling heat transfer of three R134a/RL68H mixtures (0.5 %, 1 %, and 2 % mass fractions), without nanoparticles, was measured to serve as a baseline for comparison to the RL68H4Cu mixtures.

APPARATUS

Figure 1 shows a schematic of the apparatus that was used to measure the pool boiling data of this study. More specifically, the apparatus was used to measure the liquid saturation temperature (T_s), the average pool-boiling heat flux (q''), and the wall temperature (T_w) of the test surface. The three principal components of the apparatus were the test chamber, the condenser, and the purger. The internal dimensions of the test chamber were 25.4 mm × 257 mm × 1.54 m. The test chamber was charged with approximately 7 kg of refrigerant, giving a liquid height of approximately 80 mm above the test surface. As shown in Fig. 1, the test section was visible through two opposing, flat 150 mm × 200 mm quartz windows. The bottom of the test surface was heated with high velocity (2.5 m/s) water flow. The vapor produced by liquid boiling on the test surface was condensed by the brine-cooled, shell-and-tube condenser and returned as liquid to the pool by gravity. Further details of the test apparatus can be found in Kedzierski (2002) and Kedzierski (2001a).

TEST SURFACE

Figure 2 shows the oxygen-free high-conductivity (OFHC) copper flat test plate used in this study. The test plate was machined out of a single piece of OFHC copper by electric discharge machining (EDM). A tub grinder was used to finish the heat transfer surface of the test plate with a crosshatch pattern. Average roughness measurements were used to estimate the range of average cavity radii for the surface to be between 12 μm and 35 μm. The relative standard uncertainty of the cavity measurements were approximately ± 12 %. Further information on the surface characterization can be found in Kedzierski (2001a).

MEASUREMENTS AND UNCERTAINTIES

The standard uncertainty (u_i) is the positive square root of the estimated variance u_i^2. The individual standard uncertainties are combined to obtain the expanded uncertainty (U), which is calculated from the law of propagation of uncertainty with a coverage factor. All measurement uncertainties are reported at the 95 % confidence level except where specified otherwise. For the sake of brevity, only an outline of the basic measurements and

[2] The equivalent mixture is RL68H/CuO (91.3/8.7) in terms of mass.

uncertainties is given below. Complete detail on the heat transfer measurement techniques and uncertainties can be found in Kedzierski (2000) and Appendix A, respectively.

All of the copper-constantan thermocouples and the data acquisition system were calibrated against a glass-rod standard platinum resistance thermometer (SPRT) and a reference voltage to a residual standard deviation of 0.005 K. Considering the fluctuations in the saturation temperature during the test and the standard uncertainties in the calibration, the expanded uncertainty of the average saturation temperature was no greater than 0.04 K. Consequently, it is believed that the expanded uncertainty of the temperature measurements was less than 0.1 K.

Twenty 0.5 mm diameter thermocouples were force fitted into the wells of the side of the test plate shown in Fig. 2. The heat flux and the wall temperature were obtained by regressing the measured temperature distribution of the block to the governing two-dimensional conduction equation (Laplace equation). In other words, rather than using the boundary conditions to solve for the interior temperatures, the interior temperatures were used to solve for the boundary conditions following a backward stepwise procedure given in Kedzierski (1995)[3]. Fourier's law and the fitted constants from the Laplace equation were used to calculate the average heat flux (q'') normal to and evaluated at the heat transfer surface based on its projected area. The average wall temperature (T_w) was calculated by integrating the local wall temperature (T). The wall superheat was calculated from T_w and the measured temperature of the saturated liquid (T_s). Considering this, the relative expanded uncertainty in the heat flux ($U_{q''}$) was greatest at the lowest heat fluxes, approaching 10 % of the measurement near 10 kW/m^2. In general, the $U_{q''}$ remained approximately within 3 % and 6 % for heat fluxes greater than 30 kW/m^2. The average random error in the wall superheat (U_{Tw}) was between 0.04 K and 0.1 K. Plots of $U_{q''}$ and U_{Tw} versus heat flux can be found in Appendix A.

EXPERIMENTAL RESULTS

The heat flux was varied approximately between 10 kW/m^2 and 120 kW/m^2 to simulate a range of possible operating conditions for R134a chillers. All pool-boiling tests were taken at 277.6 K saturated conditions. The data were recorded consecutively starting at the largest heat flux and descending in intervals of approximately 4 kW/m^2. The descending heat flux procedure minimized the possibility of any hysteresis effects on the data, which would have made the data sensitive to the initial operating conditions. Table 2 presents the measured heat flux and wall superheat for all the data of this study. Table 3 gives the number of test days and data points for each fluid.

The mixtures were prepared by charging the test chamber (see Fig. 1) with pure R134a to a known mass. Next, a measured mass of nanolubricant or lubricant was injected with a syringe through a port in the test chamber. The refrigerant/lubricant solution was mixed by flushing pure refrigerant through the same port where the lubricant was injected. All compositions were determined from the masses of the charged components and are given on a mass fraction basis. The maximum uncertainty of the composition measurement is

[3] For the record, Table 1 provides functional forms of the Laplace equation that were used in this study in the same way as was done in Kedzierski (1995) and in similar studies by this author.

approximately 0.02 %, e.g., the range of a 2.0 % composition is between 1.98 % and 2.02 %. Nominal or target mass compositions are used in the discussion. For example, the "actual" mass composition of the RL68H in the R134a/ RL68H (99.5/0.5) mixture was 0.53 % ± 0.02 %. Likewise, the RL68H mass fractions for R134a/ RL68H (99/1) and the R134a/ RL68H (98/2) mixtures were 1.04 % ± 0.02 % and 2.10 % ± 0.02 %, respectively. Using the same uncertainties, the nanolubricant mass fractions as tested with R134a were 0.53 %, 1.05 %, and 1.99 %.

Figure 3 is a plot of the measured heat flux (q") versus the measured wall superheat (T_w - T_s) for pure R134a at a saturation temperature of 277.6 K. The closed circles represent 13 days of boiling measurements made over a period of approximately three weeks. The solid lines shown in Fig. 3 are cubic best-fit regressions or estimated means of the data. Five of the 145 measurements were removed before fitting because they were identified as "outliers" based on having both high influence and high-leverage (Belsley et al., 1980). Table 4 gives the constants for the cubic regression of the superheat versus the heat flux for all of the fluids tested here. The residual standard deviation of the regressions - representing the proximity of the data to the mean - are given in Table 5. The dashed lines to either side of the mean represent the lower and upper 95 % simultaneous (multiple-use) confidence intervals for the mean. From the confidence intervals, the expanded uncertainty of the estimated mean wall superheat was 0.14 K and 0.06 K for superheats less than and greater than 7 K, respectively. Table 6 provides the average magnitude of 95 % multi-use confidence interval for the fitted wall superheat for all of the test data.

The effect of the pure lubricant mass fraction on R134a/lubricant pool boiling is shown in Fig. 4. Figure 4 plots the measured heat flux (q") versus the measured wall superheat (T_w - T_s) at a saturation temperature of 277.6 K for the three R134a/RL68H mixtures. Comparison of the three mean boiling curves shows that the superheats are within approximately 1 K of each other for heat fluxes between approximately 30 kW/m^2 and 90 kW/m^2. For the same heat flux range, the superheat for the pure R134a is roughly 3 K less than that for the mixtures translating into a heat transfer degradation with respect to R134a. Kedzierski (2001b) has shown that, in general, degradations due to increased lubricant mass fractions occur when the concentration induced bubble size reduction, and its accompanying loss of vapor generation per bubble, is not compensated by an increase in site density. Once a heat transfer degradation has occurred, it has been observed to continue to degrade with respect to increasing lubricant mass fraction. All the measurements shown in Fig. 4 excluding those for the (98/2) mixture where the heat flux is greater than 30 kW/m^2 are consistent with this trend. Consequently, the observation that the heat transfer degradation increases from the (99.5/0.5) mixture to the (99/1) mixture and then decreases from the (99/1) mixture to the (98/2) mixture, for heat fluxes greater than 30 kW/m^2, is unusual and unexpected. In addition, Fig. 4 and Table 6 illustrate a second unusual characteristic of the measurements in that they become more repeatable for the larger lubricant concentrations. More specifically, the average magnitude of the 95 % multi-use confidence interval for the mean superheat decreases from 0.22 K, to 0.15 K, and to 0.09 K for increasing mixture compositions of (99.5/0.5), (99/1), and (98/2), respectively. This trend is contrary to what is typically observed for increasing lubricant mass fraction refrigerant/lubricant mixture boiling heat transfer measurements, which usually exhibit increasing data scatter.

The effect of the nanolubricant mass fraction on R134a/nanolubricant pool boiling is shown in Fig. 5. Figure 5 is a plot of the measured heat flux (q'') versus the measured wall superheat ($T_w - T_s$) for the R134a/RL68H4Cu mixtures at a saturation temperature of 277.6 K. An average of 153 measurements were made for each mixture over the span of approximately a week. The means of the R134a/RL68H4Cu (99/1) and the R134a/RL68H4Cu (98/2) superheat measurements are within approximately 1 K for the entire heat flux range that was tested. For heat fluxes less than approximately 30 kW/m^2 and greater than approximately 60 kW/m^2, the R134a/RL68H4Cu (99/1) mixture mean superheat is less than that of the R134a/RL68H4Cu (98/2) mixture. For heat fluxes between these limits, the R134a/RL68H4Cu (98/2) mixture exhibits the unusual characteristic of having an enhanced boiling performance as compared to the R134a/RL68H4Cu (99/1) mixture. For most heat fluxes, the R134a/RL68H4Cu (99.5/0.5) superheat measurements, represented by the open triangles, are significantly less than those of the 99/1 and the 98/2 mixtures. For comparison, the mean of the pure R134a boiling curve is provided as a coarsely dashed line. The average expanded uncertainty of the estimated mean wall superheat for the three refrigerant/nanolubricant mixtures was 0.23 K.

A more precise comparison of the R134a/RL68H and the R134a/RL68H4Cu heat transfer performances relative to R134a and R134a/RL68H, respectively, is given in Figs. 6 and 7. Figure 6 plots the ratio of the R134a/RL68H mixture heat flux to the pure R134a heat flux (q''_{PL}/q''_p) versus the pure R134a heat flux (q''_p) at the same wall superheat. Figure 6 illustrates the influence of lubricant mass composition on the R134a/RL68H boiling curve with solid lines representing the mean heat flux ratios for each mixture. Overall, lubricant for all compositions has caused a heat transfer degradation relative to the heat transfer of pure R134a for all measured q''_p. The degradation is shown to increase with lubricant mass fraction. For example, the average heat flux ratio for the R134a/RL68H (99.5/0.5), the R134a/RL68H (99/1), and the R134a/RL68H (98/2) mixture from approximately 15 kW/m^2 to 120 kW/m^2 was 0.43, 0.37, and 0.28, respectively.[4] The minimum heat transfer degradation for each mixture (or the maximum heat transfer) is shown on Fig. 6 to be at lowest measured heat fluxes. For 20 kW/m^2, the heat flux ratio for the R134a/RL68H (99.5/0.5), the R134a/RL68H (99/1), and the R134a/RL68H (98/2) mixture is 0.62 ± 0.16, 0.58 ± 0.16, and 0.47 ± 0.12, respectively. The lubricant effect becomes more pronounced as the heat flux increases from roughly 20 kW/m^2 to 120 kW/m^2 producing heat flux ratios of approximately 0.37, 0.3, and 0.25 at 100 kW/m^2 for the R134a/RL68H (99.5/0.5), the R134a/RL68H (99/1), and the R134a/RL68H (98/2) mixtures, respectively.

Figure 7 details the effect that the CuO nanoparticles had on the R134a/RL68H boiling curves. The figure plots the ratio of the R134a/RL68H4Cu heat flux to the R134a/RL68H heat flux (q''_{CuO}/q''_{PL}) versus the R134a/RL68H4Cu mixture heat flux (q''_{CuO}) at the same wall superheat. The three different compositions are represented by three different lines where each R134a/nanolubricant mixture is compared to the R134a/pure-lubricant mixture at the same mass fraction. A heat transfer enhancement exists where the heat flux ratio is

[4] A heat transfer enhancement for the R134a/RL68H (98/2) mixture is not shown because this occurs for values of q''_p larger than what was measured. Therefore, a comparison could not be made between the fluids at the larger heat flux.

greater than one and the 95 % simultaneous confidence intervals (depicted by the shaded regions) do not include the value one. Figure 7 shows that the R134a/RL68H4Cu (99.5/0.5) mixture exhibits a significant boiling heat transfer enhancement over that of the R134a/RL68H (99.5/0.5) mixture. The heat flux ratio varies between roughly 1.5 and 3.75 for the R134a/RL68H4Cu (99.5/0.5) mixture for heat fluxes between 10 kW/m^2 and 110 kW/m^2. The R134a/RL68H4Cu (99/1) mixture shows a maximum heat flux ratio of approximately 1.54 and a region between 30 kW/m^2 and 60 kW/m^2 where no difference can be established between the two fluids because the confidence intervals include the value of one. Overall, the average heat flux ratio for the R134a/RL68H4Cu (99.5/0.5) mixture and the R134a/RL68H4Cu (99/1) mixture from approximately 10 kW/m^2 to 110 kW/m^2 was 2.4, and 1.19, respectively. The average heat flux ratio for the R134a/RL68H4Cu (98/2) mixture from approximately 10 kW/m^2 to 65 kW/m^2 was 1.12.

DISCUSSION

The heat transfer results summarized in Fig. 7 show that nanolubricants have a great potential for improving the pool boiling heat transfer of refrigerant/lubricant mixtures. However, Fig. 8 brings into question whether this enhancement is caused by an increase in thermal conductivity, as suggested in the Introduction, or some other mechanism(s). Figure 8 shows the thermal conductivity of several RL68H/CuO nanoparticle mixtures as measured with a transient line-source technique (Roder et al., 2000). Even though the thermal conductivity of CuO (20 $W/m \cdot K$)[5] is two orders of magnitude greater than that of neat RL68H (0.132 $W/m \cdot K \pm 0.001$ $W/m \cdot K$[6]), an improvement in the thermal conductivity significantly beyond that proportional to the volume fraction of the nanofluid was not obtained. For example, the volume fraction used in the boiling experiments (4 %) resulted in the nanofluid having a thermal conductivity that is roughly 5 % greater than that of the pure base fluid. This proportional improvement is disappointing compared to the 40 % improvement in thermal conductivity for a 0.4 % volume fraction achieved by Eastman et al. (2001). However, as shown in Fig. 8, the solid-liquid thermal conductivity model of Wasp (1977) confirms the measured thermal conductivity of the 4 % by volume mixture (0.139 $W/m \cdot K \pm 0.001$ $W/m \cdot K$) to within approximately 7 %.

The marginal increase in thermal conductivity of the refrigerant mixture as charged may not necessarily translate into marginal improvement of the thermal conductivity of the liquid at the heat transfer surface. The effective enhancement of the lubricant's thermal conductivity may in fact be greater than what the bulk concentration suggests because of the accumulation of nanoparticles in the lubricant excess layer that exists on the heat transfer surface. The increase in nanoparticle concentration in the excess layer was supported by observing the darkened lubricant that remained on the test surface after testing and removing the charge from the test apparatus. As a result, the thermal conductivity of the lubricant that resides on the surface and governs the boiling process may be greater than what the bulk nanoparticles concentration would suggest.

[5] Kwak and Kim (2005)

[6] This is a random uncertainty obtained solely from repeated measurements, which does not account for a possible bias error. The type B uncertainty obtained from the manufacturer was ± 0.01 $W/m \cdot K$.

In order to more closely examine the effect of thermal conductivity, Fig. 9 compares the enhancement ratio for the R134a/RL68H4Cu (99.5/0.5) mixture to those predicted by the refrigerant/lubricant mixture, pool-boiling model given in Kedzierski (2003b). The model is used to assess the effect of increased lubricant thermal conductivity on the boiling heat transfer. One prediction is presented for the charged 4 % volume fraction corresponding to a nanolubricant thermal conductivity of 0.139 W/m·K. The other prediction is presented to simulate the case where the nanoparticles accumulate to a 40 % volume fraction on the heat transfer surface giving a thermal conductivity of 0.206 W/m·K ± 0.002 W/m·K. Both predictions are at least 80 % less than the measured heat flux ratio. Consequently, the comparison demonstrates that the increased thermal conductivity of the nanofluid cannot be used to explain the entire enhancement associated with the refrigerant/nanolubricant boiling heat transfer. It appears that at most, 20 % of the enhancement may be due to increased thermal conductivity for a 40 % volume fraction excess layer. Other factors, are likely to contribute to the enhancement, for example, the particles may be inducing secondary nucleation on the bubbles and on the heat transfer surface. The particles may be agglomerating within the excess layer and acting similar to a porous surface in enhancing boiling. In addition, there may be particle-mixing effects that contribute to the heat transfer enhancement.

Future research is required to investigate the influence of the particle material, its shape, size, distribution, and concentration on refrigerant boiling performance. Not only should the bulk concentration be studied, the distribution of the concentration of the nanoparticles within a particular system should be investigated. Because of the instability of the nanoparticles in the low viscosity refrigerant, the balance between the entrainment of nanoparticles by fluid mixing (rather than Brownian motion) and the deposition of nanoparticles in the excess layer will, in part, determine the distribution of nanoparticles in a particular system. In addition, a smaller fraction of the nanoparticles may be held up in monolayers to the wetted adiabatic surfaces. Hence, several interacting mechanisms are likely to be responsible for the distribution of nanoparticles in the system and, in turn, the performance of the system. For this reason, the influence of refrigerant/nanolubricant charge, heat transfer area, and adiabatic surface area on the concentration of the nanoparticles in the lubricant excess layer should be investigated. The potential for nanoparticles to travel to the heat transfer surface by the act of boiling is dictated by the available mass of nanoparticles in the refrigerant mixture charge. Consequently, it may not be fair to compare studies at the same bulk nanoparticles concentration for two different systems because the relative refrigerant-charge-to-surface-area may differ for the two systems. Considering this, a parameter more pertinent than the bulk nanoparticles concentration for investigation may be the concentration of nanoparticles in the nanolubricant excess layer that resides on the boiling surface. Further investigation into the above effects may lead to a theory that can be used to develop nanolubricants that improve boiling heat transfer for the benefit of the refrigeration and air-conditioning industry.

CONCLUSIONS

The effect of CuO nanoparticles on the boiling performance of R134a/polyolester mixtures on a roughened, horizontal flat surface was investigated. A nanolubricant containing CuO nanoparitcles at 4 % volume fraction with a polyolester lubricant was mixed with R134a at three different mass fractions. For the 0.5 % nanolubricant mass fraction, the nanoparticles

caused a heat transfer enhancement relative to the heat transfer of pure R134a/polyolester (99.5/0.5) between 50 % and 275 %. A smaller enhancement was observed for the R134a/nanolubricant (99/1) mixture, which had a heat flux that was on average 19 % larger than that of the R134a/polyolester (99/1) mixture. Further increase in the nanolubricant mass fraction to 2 % resulted in a still smaller boiling heat transfer improvement of approximately 12 % on average for the R134a/nanolubricant (98/2) mixture. The measurements illustrate that the performance improvement decreases with increasing lubricant concentration. In other words, nanoparticles are less likely to be of benefit where they are needed most. However, if a system can be designed to maintain a small lubricant concentration in the evaporator, significant performance improvements can be expected.

Although the nanoparticles increased the thermal conductivity of the lubricant, the increase in thermal conductivity appears to be responsible for only a small portion (potentially 20 %) of the boiling heat transfer enhancement. Other effects, in particular, secondary nucleation and particle mixing may contribute more significantly to the enhancement of the refrigerant/lubricant boiling heat transfer with nanoparticles.

ACKNOWLEDGEMENTS
This work was funded by NIST. Thanks go to the following NIST personnel for their constructive criticism of the first draft of the manuscript: Mr. B. Dougherty, and Dr. P. Domanski. Thanks go to Prof. A. Jacobi of the University of Illinois at Urbana-Champaign for his constructive criticism of the second draft of the manuscript. Furthermore, the authors extend appreciation to W. Guthrie and Mr. A. Heckert of the NIST Statistical Engineering Division for their consultations on the uncertainty analysis. Some boiling heat transfer measurements were taken by Mr. David Wilmering of KT Consultants. The RL68H (EMKARATE RL 68H) was donated by Dr. S. Randles of Uniqema. The RL68H4Cu was manufactured by Nanophase Technologies with a copper (II) oxide and dispersant in RL68H especially for NIST.

NOMENCLATURE

English Symbols

A_n	regression constant in Table 4 n=0,1,2,3
C_o	viscometer calibration constant, $\mu m^2 \cdot s^{-1}$
g	gravitational acceleration, $m\ s^{-2}$
k	thermal conductivity, $W \cdot K^{-1}\ m^{-1}$
l	capillary rise height, m
L_y	length of test surface (Fig. 2), m
M	mass, kg
q"	average wall heat flux, $W \cdot m^{-2}$
r	radius of capillary tube, m
T	temperature, K
T_w	temperature at roughened surface, K
U	expanded uncertainty
u_i	standard uncertainty
V	volume, m^3
X	model terms given in Table 2

Greek symbols

ΔT	temperature difference, K
ΔT_s	wall superheat: T_w - T_s, K
$\Delta\rho$	difference between liquid and vapor density, $kg \cdot m^{-3}$
ν	kinematic viscosity, $m^2 \cdot s^{-1}$
ρ	liquid density, $kg \cdot m^{-3}$
σ	surface tension, $kg \cdot s^{-2}$
ϕ	volume fraction

English Subscripts

CuO	R134a/RL68H4Cu mixture
i	initial volume
l	neat lubricant
L	nanolubricant
np	nanoparticles
p	pure R134a
PL	R134a/RL68H mixture
q"	heat flux
s	saturated state
t	target volume
T	total volume
Tw	wall temperature
w	wall, heat transfer surface
+	added volume

REFERENCES

Adamson, A. W., and Gast, A. P., 1997, Physical Chemistry of Surfaces, Interscience Publ., New York, 6th Ed., p. 11.

Bang, I. C. and, Chang, S. H., 2004, "Boiling Heat Transfer Performance and Phenomena of Al_2O_3–Water Nanofluids From a Plain Surface in a Pool," Proceedings of ICAPP, Pittsburgh, PA, pp. 1437-1443.

Belsley, D. A., Kuh, E., and Welsch, R. E., 1980, Regression Diagnostics: Identifying Influential Data and Sources of Collinearity, New York: Wiley.

Eastman, J. A, Choi, S. U. S., Li, S., Yu, W., and Thompson, L. J., 2001, "Anomalously Increased Effective Thermal Conductivities of Ethylene Glycol-Based Nanofluids Containing Copper Nanoparticles," Appl. Phys. Lett. 78, p.718-720.

Incropera, F. P., and DeWitt, D. P., 1985, Fundamentals of Heat and Mass Transfer, 2nd ed., John Wiley & Sons, New York.

Kedzierski, M. A., 2003a, "A Semi-Theoretical Model for Predicting R123/Lubricant Mixture Pool Boiling Heat Transfer," Int. J. Refrigeration, Vol. 26, pp. 337-348.

Kedzierski, M. A., 2003b, "Improved Thermal Boundary Layer Parameter For Semi-Theoretical Refrigerant/Lubricant Pool Boiling Model," Proceedings of Int. Congress of Refrigeration, ICR0504, Washington, DC.

Kedzierski, M. A., 2002, "Use of Fluorescence to Measure the Lubricant Excess Surface Density During Pool Boiling," Int. J. Refrigeration, Vol. 25, pp.1110-1122.

Kedzierski, M. A., 2001a, "Use of Fluorescence to Measure the Lubricant Excess Surface Density During Pool Boiling," NISTIR 6727, U.S. Department of Commerce, Washington, D.C.

Kedzierski, M. A., 2001b, "The Effect of Lubricant Concentration, Miscibility and Viscosity on R134a Pool Boiling" Int. J. Refrigeration, Vol. 24, No. 4., pp. 348-366.

Kedzierski, M. A., 2000, "Enhancement of R123 Pool Boiling by the Addition of Hydrocarbons," Int. J. Refrigeration, Vol. 23, pp. 89-100.

Kedzierski, M. A., 1995, "Calorimetric and Visual Measurements of R123 Pool Boiling on Four Enhanced Surfaces," NISTIR 5732, U.S. Department of Commerce, Washington.

Kwak, K., and Kim, C., 2005, "Viscosity and Thermal Conductivity of Copper Oxide nanofluid Dispersed in Ethylene Glycol, Korea-Australia Rheology J., Vol. 17, No. 2, pp. 35-40.

Reid, R. C., Prausnitz, J. M., and Sherwood, T. K., 1977, The Properties of Gases and Liquids, 3rd ed., McGraw-Hill, NY, p. 87.

Roder, H. M., Perkins, R. A., Laesecke, A., and Nieto de Castro, C. A., 2000, "Absolute Steady-State Thermal Conductivity Measurements by Use of a Transient Hot-Wire System," J. Res. Natl. Inst. of Stand. and Technol., Vol. 105, No. 2, pp 221-253.

Sung, L., 2006, Private Communications, National Institute of Standards and Technology, Building and Fire Research Laboratory, Gaithersburg, MD.

Wasp, F. J., 1977, "Solid-Liquid Flow Slurry Pipeline Transportation, Trans., Tech. Pub., Berlin.

Wen, D, and Ding, Y., 2005, "Experimental Investigation into the Pool Boiling Heat Transfer of Aqueous Based γ-Alumina Nanofluids," J. of Nanoparticle Research, Vol. 7, pp. 265-274.

You, S. M., Kim, J. H., and Kim, K. H., 2003, "Effect of Nanoparticles on Critical Heat Flux of Water in Pool Boiling Heat Transfer," Applied Physics Letter, 83 (16) pp. 375-377.

Table 1 Conduction model choice

X_0= constant (all models) X_1= x X_2= y X_3= xy $X_4=x^2-y^2$ $X_5= y(3x^2-y^2)$ $X_6= x(3y^2-x^2)$ $X_7= x^4+y^4-6(x^2)y^2$ $X_8= yx^3-xy^3$	
Fluid	Most frequent models
Pure R134a (file: nan134.dat)	X_1,X_3 (73 of 145) 50 % X_1,X_2 (61 of 145) 42 %
R134a/RL68H (99.5/0.5) (file: RL685.dat)	X_1,X_3 (70 of 186) 38 % X_1,X_2 (53 of 186) 28 % X_1,X_2,X_3 (16 of 186) 9 % X_1,X_2,X_5 (15 of 186) 8 %
R134a/RL68H (99/1) (file: RL681.dat)	X_1,X_2 (48 of 68) 70 % X_1,X_2,X_4,X_6 (11 of 68) 17 %
R134a/RL68H (98/2) (file: RL682.dat)	X_1,X_2,X_3,X_4,X_6 (148 of 192) 77 % X_1,X_2 (15 of 192) 8 % X_1,X_2,X_4 (12 of 192) 6 % X_1,X_3,X_4,X_6 (12 of 192) 6 %
R134a/RL68H4Cu (99.5/0.5) (file: RL4Cu5.dat)	X_1,X_2,X_4,X_6 (66 of 132) 50 % X_1,X_2,X_4 (41 of 132) 31 % X_1,X_2 (26 of 132) 19 %
R134a/RL68H4Cu (99/1) (file: RL4Cu1.dat)	X_1,X_2,X_4 (61 of 157) 39 % X_1,X_2,X_4,X_6 (54 of 157) 35 % X_1,X_2 (31 of 157) 20 %
R134a/RL68H4Cu (98/2) (file: RL4Cu2.dat)	X_1,X_2,X_3 (82 of 170) 48 % X_1,X_2,X_3,X_5 (30 of 170) 18 % X_1,X_3 (24 of 170) 14 % X_1,X_2 (17 of 170) 10 %

Table 2 Pool boiling data

Pure R134a
File: NAN134.dat

ΔT_s (K)	q'' (W/m^2)
8.92	126104.
8.79	119028.
8.59	106475.
8.43	99070.
8.28	91217.
8.01	82705.
7.64	69801.
7.28	60015.
6.85	50199.
6.50	44511.
6.19	39901.
5.67	31859.
4.77	20893.
4.25	15759.
3.82	12669.
8.73	130507.
8.62	122030.
8.51	114036.
8.39	106353.
8.24	98914.
8.08	91180.
7.91	84209.
7.70	76344.
7.46	68271.
7.20	60806.
6.84	51759.
6.49	44281.
6.05	36180.
5.58	29364.
5.03	22199.
4.17	14172.
3.34	9814.
8.62	126906.
8.47	116864.
8.29	108305.
8.09	97927.
7.85	86807.
7.71	81105.
7.57	75561.
7.27	65138.
6.73	50435.
8.92	127596.
8.73	117731.
8.50	105501.
8.31	96894.
8.14	88757.
7.94	80277.
7.29	57205.
6.70	42432.
5.87	27905.
8.88	122952.
8.58	109658.
8.30	96066.
8.04	84007.
7.57	66907.
7.03	50278.
6.61	40074.
5.94	27932.
5.11	17791.
9.04	130031.
8.69	116715.
8.15	91440.
7.87	80278.
7.39	63193.
7.01	51846.
6.49	38993.
5.74	25263.
4.99	16917.
8.97	124136.
8.67	111439.
8.30	98564.
7.95	84354.
7.52	69117.
6.97	52438.
6.47	40246.
5.71	26725.
4.51	14899.
8.95	126301.
8.58	110232.
8.22	95839.
7.74	77856.
7.34	64277.
6.85	50734.
6.33	38495.
5.48	24416.
4.27	13582.
9.06	138038.
8.50	113047.
8.27	102662.
8.04	92250.
7.68	78416.
7.18	61740.
6.43	42351.
5.90	32295.
5.11	21158.
9.08	125354.
8.79	114612.
8.58	107058.
8.36	98699.
8.21	92508.
8.05	86679.
7.86	78617.
7.68	72797.
7.35	61711.
7.01	52569.
6.65	43745.
6.44	39244.
6.12	33020.
5.75	26675.
5.10	19366.
4.42	14315.
9.23	129754.
8.89	119950.
8.65	111371.
8.45	104257.
8.20	95214.
8.03	88745.
7.76	78490.
7.54	71987.
7.34	65568.
6.99	55133.
6.74	48295.
6.41	40600.
6.04	33478.
5.79	28819.
5.32	22439.
4.68	16512.
4.02	12126.
9.08	126898.
8.89	119389.
8.64	109873.
8.44	102531.
8.24	94776.
8.01	86955.
7.87	82399.
7.66	75306.
7.30	63501.
7.02	54784.
6.75	47883.
6.42	40001.
6.07	33381.
5.62	26016.
5.04	19027.
4.41	14216.
3.65	10334.

R134a/RL68H (99.5/0.5)
File: RL685.dat

ΔT_s (K)	q'' (W/m^2)
10.41	125461.
10.09	117289.
9.82	109225.
9.55	98358.
9.52	91624.
9.53	84267.
9.58	72981.
9.51	65377.
9.27	56853.
8.79	47343.
8.85	47278.
8.77	38900.
8.76	31930.
7.62	25182.
6.67	19668.
5.55	14154.
4.38	10401.
10.64	116069.
10.27	110599.
9.98	100115.
10.17	91232.
10.29	91094.
10.32	91375.

10.33	90476.
10.36	90320.
10.41	89728.
10.55	90939.
10.44	91270.
10.35	90233.
10.43	90408.
10.44	91518.
10.43	90661.
10.39	90783.
10.25	83003.
10.91	123338.
10.61	123991.
10.33	124434.
10.09	123731.
9.93	122460.
9.71	124093.
9.81	122523.
9.81	122964.
9.88	122758.
11.83	124963.
10.63	122392.
10.01	125262.
9.85	124800.
9.79	124447.
9.78	124857.
10.25	101381.
10.53	100100.
10.62	99685.
11.06	121789.
10.39	110647.
10.41	110453.
10.37	111313.
10.48	109214.
10.81	101046.
10.81	100335.
10.78	100504.
10.74	101889.
11.52	114620.
9.01	31346.
8.61	31682.
8.29	31432.
8.01	31367.
7.92	31200.
7.94	31877.
8.73	41245.
8.70	41025.
8.68	41310.
9.37	54189.
9.32	53486.
9.35	53874.
10.01	69882.
10.71	85442.
10.02	69569.
10.74	85289.
10.72	117490.
10.55	89892.
10.76	90368.
10.76	89757.
10.78	89430.
10.52	76064.
10.53	74333.
10.41	75353.
9.29	52566.
9.32	53737.

8.52	42095.
8.58	42005.
8.64	41953.
11.08	116281.
10.51	109510.
9.66	110884.
9.65	111548.
9.65	110644.
9.70	95978.
10.36	95059.
10.43	95029.
10.43	94190.
10.62	79303.
10.62	78988.
10.58	78967.
9.65	59256.
9.63	59493.
9.66	115942.
9.47	115817.
9.45	115446.
9.43	116102.
9.82	101375.
9.79	101447.
9.89	101632.
10.58	80370.
10.51	83137.
10.10	69612.
9.98	69519.
9.89	68735.
9.94	68481.
9.60	63125.
9.55	62877.
9.57	62833.
9.08	53290.
9.11	52372.
10.69	108075.
10.42	108081.
9.51	107191.
10.32	77311.
10.54	78551.
10.56	80934.
8.90	34451.
8.81	36837.
8.65	37225.
7.51	27878.
7.41	27849.
7.31	27864.
7.27	27338.
7.17	27023.
9.97	118979.
9.90	98160.
10.19	98735.
10.22	99564.
10.28	99233.
10.64	81195.
10.72	81282.
10.64	79004.
9.99	61334.
10.89	115820.
9.52	61465.
9.38	65648.
9.45	66079.
8.35	37041.
8.26	37629.
8.26	37613.

6.26	19940.
5.21	12965.
10.13	126231.
9.80	84883.
9.84	85440.
9.91	84946.
10.01	73115.
9.97	73398.
9.99	73437.
9.32	54567.
9.23	54394.
9.22	54900.
8.16	33901.
8.07	34073.
8.00	33965.
5.81	16579.
5.78	16880.
10.26	114713.
10.06	88189.
10.06	88985.
10.02	89430.
9.99	70106.
9.94	68598.
9.90	68983.
9.07	43312.
8.98	43557.
8.95	43212.
8.04	35039.
7.94	35399.
7.98	34504.
6.98	26646.
5.53	15057.
4.42	11080.

R134a/RL68H (99/1)
File: RL681.dat

ΔT_s (K)	q'' (W/m^2)
11.45	114670.
11.48	114253.
11.37	101278.
11.28	93385.
11.06	84673.
10.76	76916.
10.39	69048.
9.99	59964.
9.74	53229.
9.31	43447.
9.02	36925.
8.43	30041.
7.79	24720.
6.98	19617.
6.19	15805.
5.13	11493.
11.61	117238.
11.52	109067.
11.55	101159.
11.40	92569.
11.14	85753.
10.87	77917.
10.65	72768.
10.37	66045.
10.13	59958.

9.79	51877.
9.47	43112.
9.21	38451.
8.65	31184.
8.08	26866.
7.45	22486.
6.45	16995.
5.38	12742.
11.33	111594.
11.38	104916.
11.22	95263.
11.09	88873.
10.70	78358.
10.35	72485.
10.09	67134.
9.76	59670.
9.44	53291.
9.17	46083.
8.84	39211.
8.43	32932.
7.96	28150.
7.43	23881.
6.74	19409.
5.85	14945.
4.80	11088.
11.39	116661.
11.22	107363.
11.18	98750.
11.18	92532.
11.07	85485.
10.88	78025.
10.66	71220.
10.37	65212.
10.11	60634.
9.75	51898.
9.30	42407.
8.91	36174.
8.35	29873.
7.75	25073.
6.82	19068.
5.87	14832.
4.92	11145.
3.87	8484.

R134a/RL68H (98/2)
File: RL682.dat

ΔT_s (K)	q'' (W/m^2)
10.46	120365.
10.45	115838.
10.41	111220.
10.32	94618.
10.39	97658.
10.29	90814.
10.32	92784.
10.34	92810.
10.18	79753.
10.15	79841.
10.16	81082.
9.94	69921.
9.94	70162.
9.91	70304.
9.67	59011.
9.63	58948.
9.61	59241.
9.34	48700.
9.29	48182.
9.23	47451.
8.88	35719.
8.84	33420.
8.78	33779.
8.53	28958.
8.52	28533.
8.52	28117.
7.97	20339.
7.94	19897.
7.90	19509.
7.09	14308.
6.79	13139.
10.11	96882.
10.21	101028.
10.25	104081.
10.16	96491.
10.18	96990.
10.22	98340.
10.26	92205.
10.31	93439.
10.36	94510.
10.18	80878.
10.19	81197.
10.21	81995.
9.91	67986.
9.89	67802.
9.87	68453.
9.59	56984.
9.57	56757.
9.56	57119.
9.31	47737.
9.27	47201.
9.24	46919.
8.90	37682.
8.85	36516.
8.73	32965.
8.49	27176.
8.46	26594.
8.44	26820.
8.03	20650.
8.02	20603.
8.01	20637.
6.97	13807.
6.91	13468.
6.90	13458.
4.37	7773.
4.13	7814.
10.38	116228.
10.36	114533.
10.32	112413.
10.03	93005.
10.03	90636.
10.04	89940.
9.91	79400.
9.93	79285.
9.97	79490.
9.77	67901.
9.73	67241.
9.71	67796.
9.53	58973.
9.50	58434.
9.50	58730.
9.27	49772.
9.25	49249.
9.22	48154.
8.97	40005.
8.97	40118.
8.97	40693.
8.55	28219.
8.52	27593.
8.52	27297.
7.97	19489.
7.93	19342.
7.95	19757.
7.10	13514.
7.07	13348.
7.09	13330.
5.12	9463.
4.97	9221.
10.35	113634.
10.39	113879.
10.38	113399.
10.21	101492.
10.20	100433.
10.20	99352.
10.08	86806.
10.10	85998.
10.13	85876.
9.99	74165.
9.99	73536.
9.97	73612.
9.67	59843.
9.63	59155.
9.60	58851.
9.29	48030.
9.24	48251.
9.21	48237.
8.91	38365.
8.90	38280.
8.90	38433.
8.56	28864.
8.54	28522.
8.52	28082.
8.03	20657.
7.98	20000.
7.98	20026.
6.99	13522.
6.88	13219.
6.90	13323.
4.75	8496.
4.52	8336.
10.39	113340.
10.38	111810.
10.36	109427.
10.22	100505.
10.19	98596.
10.21	97769.
10.08	83945.
10.07	83114.
10.10	83292.
9.99	73887.
9.99	74076.
10.00	74565.
9.69	62807.
9.67	62988.

9.65	63454.
9.40	52781.
9.37	52792.
9.35	52793.
9.12	44736.
9.10	44631.
9.10	44755.
8.81	34764.
8.76	34063.
8.76	34093.
8.33	24570.
8.28	23925.
8.27	23887.
7.64	16725.
7.60	16375.
7.62	17454.
5.90	10924.
5.66	10706.
10.33	96303.
10.34	94383.
10.31	93085.
10.11	79719.
10.11	78470.
10.14	78057.
9.91	67703.
9.87	67670.
9.83	67582.
9.53	55465.
9.50	55634.
9.50	56202.
9.23	45653.
9.19	44948.
9.14	45623.
8.85	35942.
8.86	36362.
8.84	36780.
8.34	24576.
8.37	24673.
8.39	24993.
7.74	17522.
7.70	17398.
7.72	17517.
6.49	11613.
6.34	11481.
6.29	11206.
4.80	8877.
4.67	8884.
4.69	8920.

R134a/RL68H4Cu (99.5/0.5)
File: RL4Cu5.dat

ΔT_s (K)	q'' (W/m^2)
8.58	108670.
7.98	101295.
7.71	94268.
7.24	84389.
7.14	77994.
7.12	73189.
6.89	59731.
7.57	52222.
7.14	43333.
6.74	37432.
6.39	32012.
6.18	28581.
5.63	23208.
4.89	17594.
4.24	15345.
3.45	11017.
8.07	104134.
7.49	98239.
7.08	90736.
6.86	83594.
6.76	76379.
6.91	70628.
6.96	63820.
7.11	56794.
6.88	51101.
6.55	45204.
6.49	35966.
6.24	32460.
5.90	28561.
5.15	20877.
4.43	17539.
3.75	13200.
7.71	108174.
7.16	101751.
6.87	95097.
6.79	88910.
6.85	82367.
6.86	74585.
7.35	69317.
7.43	60356.
7.11	54639.
6.69	47786.
6.33	40530.
5.98	34347.
5.73	30130.
5.32	25229.
4.71	21116.
4.11	16094.
3.48	11974.
7.23	97257.
7.04	88884.
6.97	76461.
6.92	82271.
7.23	68989.
7.89	62465.
8.15	57984.
7.82	51489.
7.54	45596.
7.03	37402.
6.79	30262.
6.32	25728.
5.54	21812.
4.88	17308.
3.85	11820.
8.46	109658.
7.98	102696.
7.69	95626.
7.52	89791.
7.37	82639.
7.58	76129.
7.83	68624.
8.21	60228.
8.16	54231.
7.75	46416.
7.46	37082.
6.85	29355.
6.42	25715.
5.63	19775.
4.87	16983.
3.93	11987.
8.10	112782.
7.74	106076.
7.65	100674.
7.65	93818.
7.56	84705.
7.67	76848.
7.86	70397.
8.01	63698.
7.98	57635.
7.98	52079.
7.59	44632.
7.37	37876.
7.03	31737.
6.62	27346.
5.97	21934.
5.07	17898.
4.15	12991.
8.10	113418.
7.75	107131.
7.49	100701.
7.47	92226.
7.70	84174.
7.70	78430.
7.62	71396.
7.77	67305.
7.80	57584.
8.21	53149.
7.99	45743.
7.69	36808.
7.36	29231.
7.08	24901.
6.37	20541.
5.25	16369.
4.02	11383.
7.79	123100.
7.36	113999.
7.05	105138.
6.84	96025.
6.72	86175.
6.76	79422.
6.90	72075.
7.18	64916.
7.55	60155.
7.60	49001.
7.56	42658.
7.40	35804.
7.33	27925.
6.73	22862.
5.92	20134.
4.91	15249.
3.99	11532.
3.22	9701.

R134a/RL68H4Cu (99/1)
File: RL4Cu1.dat

ΔT_s (K)	q'' (W/m^2)

(K)	
10.60	103166.
10.21	93530.
10.09	86311.
9.88	78804.
9.69	71499.
9.59	64194.
9.31	56611.
9.23	50457.
9.07	42082.
8.82	37123.
8.37	32224.
7.61	26896.
7.04	23433.
5.96	19523.
5.01	15069.
4.18	11702.
10.33	101030.
9.99	94207.
9.80	86567.
9.54	78575.
9.54	71329.
9.29	62666.
9.20	55782.
9.01	48927.
8.95	42343.
8.74	37814.
8.29	34129.
7.70	29346.
7.15	25624.
6.48	21547.
5.69	17369.
4.91	15376.
4.06	11667.
10.48	101465.
10.06	94378.
9.90	88678.
9.76	82513.
9.53	73434.
9.53	67989.
9.34	59422.
9.29	54735.
9.12	49853.
8.73	42361.
8.43	36045.
7.90	30783.
7.32	27021.
6.31	20422.
5.32	17538.
4.47	13486.
3.53	9817.
11.22	101906.
10.74	93607.
10.58	86294.
10.37	78433.
10.19	70480.
10.41	70114.
10.04	60758.
9.80	54318.
9.50	48886.
9.22	43934.
8.71	36869.
8.52	33927.
7.80	28512.
7.16	24330.
6.51	20635.
5.60	17757.
4.75	13868.
11.74	102607.
11.37	96498.
11.06	88918.
10.83	81607.
10.63	75313.
10.37	68995.
10.15	62096.
10.00	55724.
9.65	48422.
9.34	41191.
8.73	34270.
8.14	28910.
7.60	25166.
7.05	22071.
6.17	19254.
5.22	14892.
4.26	11183.
11.92	103832.
11.50	95600.
11.19	86633.
10.99	78660.
10.70	70602.
10.47	64027.
10.26	57898.
9.88	50591.
9.67	44603.
9.33	38714.
9.16	35229.
8.32	28781.
7.71	25031.
7.22	22212.
6.56	20737.
5.48	15659.
4.38	11336.
12.11	103981.
11.80	104318.
11.64	100707.
11.36	93045.
11.31	84163.
11.10	78904.
10.94	73910.
10.75	68555.
10.51	63359.
10.20	55681.
10.04	49678.
9.67	43417.
9.11	34916.
8.52	29894.
7.71	24695.
6.91	22266.
6.30	19068.
5.37	14908.
4.43	11307.
8.58	35618.
7.89	29237.
10.28	104159.
9.85	97269.
9.68	89609.
9.80	84302.
9.39	73363.
9.40	67565.
9.70	60493.
9.55	54493.
9.48	47516.
9.21	42770.
7.16	25064.
6.56	21456.
5.71	17132.
4.87	15067.
4.20	12111.
10.44	102008.
10.11	101694.
10.20	102387.
9.77	94590.
9.47	87837.
9.42	81093.
9.34	73906.
9.31	65603.
9.21	56173.
9.13	49493.
9.00	43429.
8.56	36691.
8.11	31744.
7.47	27562.
6.77	23176.
6.90	23940.
6.32	20761.
5.48	18296.
4.66	14140.
3.36	9030.

R134a/RL68H4Cu (98/2)
File: RL4Cu2.dat

ΔT_s (K)	q'' (W/m^2)
10.46	117375.
10.72	116499.
10.87	107367.
10.87	107367.
11.14	105427.
11.03	98635.
11.08	97650.
11.13	97721.
10.87	90341.
10.87	90912.
10.88	90957.
10.70	84665.
10.68	84396.
10.63	83865.
10.38	77812.
10.35	77220.
9.89	70267.
9.66	71057.
11.02	106456.
9.75	71093.
9.10	63377.
9.16	63605.
8.24	38542.
8.24	38282.
8.25	38343.
8.09	33614.
8.13	33300.
8.14	33219.
7.85	29422.
7.84	29130.

7.87	28847.
7.40	24414.
7.38	24237.
7.38	24019.
7.07	21693.
7.07	21584.
12.38	115121.
12.41	114192.
12.38	111421.
12.11	100519.
12.15	101108.
12.19	100852.
11.79	92992.
11.72	92736.
11.68	92689.
11.28	82992.
11.33	82498.
11.34	82218.
10.67	74378.
10.49	73403.
10.62	73787.
10.13	67387.
9.97	69014.
9.95	69272.
9.73	59182.
9.52	60427.
9.51	60576.
9.52	60679.
9.83	46661.
12.66	108402.
12.71	109366.
12.70	109431.
12.03	97660.
11.99	97448.
11.98	97568.
11.46	88727.
11.40	88896.
11.42	89543.
10.83	79243.
10.80	78999.
10.75	79352.
10.07	70410.
10.01	71980.
10.16	72631.
9.41	62404.
9.38	62431.
9.41	62499.
8.83	50141.

8.87	49166.
8.87	48648.
8.56	41777.
8.59	41303.
8.65	41110.
8.09	30369.
8.07	29521.
7.98	28324.
7.18	21028.
7.21	20786.
7.28	20909.
4.09	7804.
3.78	7242.
3.64	6897.
3.64	6897.
3.64	6897.
3.64	6897.
3.64	6897.
10.57	118327.
11.08	117679.
11.57	113229.
11.36	101711.
11.63	102424.
11.79	103235.
11.47	91806.
11.55	91835.
11.61	92244.
11.24	84466.
11.27	84462.
11.30	84451.
10.81	76156.
10.79	76537.
10.75	76372.
10.11	67364.
9.95	66474.
9.87	66244.
9.34	57958.
9.14	57810.
9.17	56532.
8.90	50334.
8.95	50320.
8.96	50228.
8.50	39834.
8.55	39828.
8.55	39438.
8.05	28784.
8.08	28331.
7.31	21831.

7.26	20580.
7.22	20257.
6.40	15790.
6.41	15744.
6.47	15812.
4.52	8449.
3.82	7355.
3.65	6977.
12.04	96718.
12.23	98927.
12.40	102452.
11.94	89763.
12.04	90371.
12.13	91078.
11.71	80889.
11.70	81324.
11.71	81709.
11.13	71608.
11.02	72162.
11.03	72141.
10.47	63398.
10.29	63570.
10.21	63573.
9.66	54444.
9.58	55300.
9.65	56206.
9.23	45690.
9.35	44895.
9.36	44622.
8.73	33685.
8.80	32253.
8.86	31517.
8.04	25273.
7.98	24674.
7.97	24231.
6.84	17476.
6.74	16696.
6.79	16702.
5.52	11747.
5.35	11409.
5.35	11352.
4.17	7825.
3.89	7495.
3.83	7362.

Table 3 Number of test days and data points

Fluid (% mass fraction)	Number of days	Number of data points
Pure R134a 3 K ≤ ΔT_s ≤ 9 K	13	145
R134a/RL68H (99.5/0.5) 4.3 K ≤ ΔT_s ≤ 10.2 K	14	186
R134a/RL68H (99/1) 4.6 K ≤ ΔT_s ≤ 11.3 K	4	68
R134a/RL68H (98/2) 4 K ≤ ΔT_s ≤ 10.5 K	6	192
R134a/RL68H4Cu (99.5/0.5) 3.4 K ≤ ΔT_s ≤ 8.2 K	8	132
R134a/RL68H4Cu (99/1) 3.5 K ≤ ΔT_s ≤ 10.7 K	9	157
R134a/RL68H4Cu (98/2) 3.5 K ≤ ΔT_s ≤ 12 K	5	170

Table 4 Estimated parameters for cubic boiling curve fits for plain copper surface

$\Delta T_s = A_0 + A_1 q" + A_2 q"^2 + A_3 q"^3$

ΔT_s in Kelvin and $q"$ in W/m^2

Fluid	A_o	A_1	A_2	A_3
Pure R134a				
3 K ≤ ΔT_s ≤ 7 K	1.41341	2.70461×10^{-4}	-5.22703×10^{-9}	3.94517×10^{-14}
7 K ≤ ΔT_s ≤ 9 K	3.99702	7.78356×10^{-5}	-4.89337×10^{-10}	1.44222×10^{-15}
R134a/RL68H (99.5/0.5)				
4.3 K ≤ ΔT_s ≤ 9.5 K	1.66769	3.15055×10^{-4}	-4.19310×10^{-9}	1.77327×10^{-14}
9.5 K ≤ ΔT_s ≤ 10.2 K	1.04922	2.64699×10^{-4}	-2.48124×10^{-9}	7.59925×10^{-15}
R134a/RL68H (99/1)				
4.6 K ≤ ΔT_s ≤ 9.7 K	1.00155	4.33942×10^{-4}	-7.83196×10^{-9}	5.15712×10^{-14}
9.7 K ≤ ΔT_s ≤ 11.3 K	9.14630	-3.72774×10^{-5}	1.28138×10^{-9}	-6.85804×10^{-15}
R134a/RL68H (98/2)				
4 K ≤ ΔT_s ≤ 8.5 K	-5.53159	1.77713×10^{-3}	-7.97232×10^{-8}	1.23223×10^{-12}
8.5 K ≤ ΔT_s ≤ 10.5 K	7.09007	5.83429×10^{-5}	-2.74470×10^{-10}	1.13436×10^{-16}
R134a/RL68H4Cu (99.5/0.5)				
3.4 K ≤ ΔT_s ≤ 8.2 K	7.52004×10^{-1}	3.15645×10^{-4}	-4.69784×10^{-9}	2.20673×10^{-14}
R134a/RL68H4Cu (99/1)				
3.5 K ≤ ΔT_s ≤ 9 K	6.0058×10^{-1}	3.28260×10^{-4}	-1.31501×10^{-9}	-4.42454×10^{-14}
9 K ≤ ΔT_s ≤ 10.7 K	4.51615	1.84658×10^{-4}	-2.18782×10^{-9}	9.58136×10^{-15}
R134a/RL68H4Cu (99/2)				
3.5 K ≤ ΔT_s ≤ 8.75 K	3.00385×10^{-2}	6.44828×10^{-4}	-1.79772×10^{-8}	1.78650×10^{-13}
8.75 K ≤ ΔT_s ≤ 12 K	7.65055	-2.18447×10^{-5}	1.37521×10^{-9}	-7.45213×10^{-15}

Table 5 Residual standard deviation of ΔT_s

Fluid	u (K)
Pure R134a	
3 K ≤ ΔT_s ≤ 7 K	0.15
7 K ≤ ΔT_s ≤ 9 K	0.10
R134a/RL68H (99.5/0.5)	
4.3 K ≤ ΔT_s ≤ 9.5 K	0.28
9.5 K ≤ ΔT_s ≤ 10.2 K	0.41
R134a/RL68H (99/1)	
4.6 K ≤ ΔT_s ≤ 9.7 K	0.13
9.7 K ≤ ΔT_s ≤ 11.3 K	0.12
R134a/RL68H (98/2)	
4 K ≤ ΔT_s ≤ 8.5 K	0.09
8.5 K ≤ ΔT_s ≤ 10.5 K	0.07
R134a/RL68H4Cu (99.5/0.5)	
3.4 K ≤ ΔT_s ≤ 8.2 K	0.45
R134a/RL68H4Cu (99/1)	
3.5 K ≤ ΔT_s ≤ 9 K	0.23
9 K ≤ ΔT_s ≤ 10.7 K	0.51
R134a/RL68H4Cu (99/2)	
3.5 K ≤ ΔT_s ≤ 8.75 K	0.16
8.75 K ≤ ΔT_s ≤ 12 K	0.43

Table 6 Average magnitude of 95 % multi-use confidence interval for mean $T_w - T_s$ (K)

Fluid	u (K)
Pure R134a	
3 K ≤ ΔT_s ≤ 7 K	0.14
7 K ≤ ΔT_s ≤ 9 K	0.06
R134a/RL68H (99.5/0.5)	
4.3 K ≤ ΔT_s ≤ 9.5 K	0.22
9.5 K ≤ ΔT_s ≤ 10.2 K	0.22
R134a/RL68H (99/1)	
4.6 K ≤ ΔT_s ≤ 9.7 K	0.15
9.7 K ≤ ΔT_s ≤ 11.3 K	0.14
R134a/RL68H (98/2)	
4 K ≤ ΔT_s ≤ 8.5 K	0.09
8.5 K ≤ ΔT_s ≤ 10.5 K	0.04
R134a/RL68H4Cu (99.5/0.5)	
3.4 K ≤ ΔT_s ≤ 8.2 K	0.26
R134a/RL68H4Cu (99/1)	
3.5 K ≤ ΔT_s ≤ 9 K	0.18
9 K ≤ ΔT_s ≤ 10.7 K	0.34
R134a/RL68H4Cu (99/2)	
3.5 K ≤ ΔT_s ≤ 8.75 K	0.15
8.75 K ≤ ΔT_s ≤ 12 K	0.24

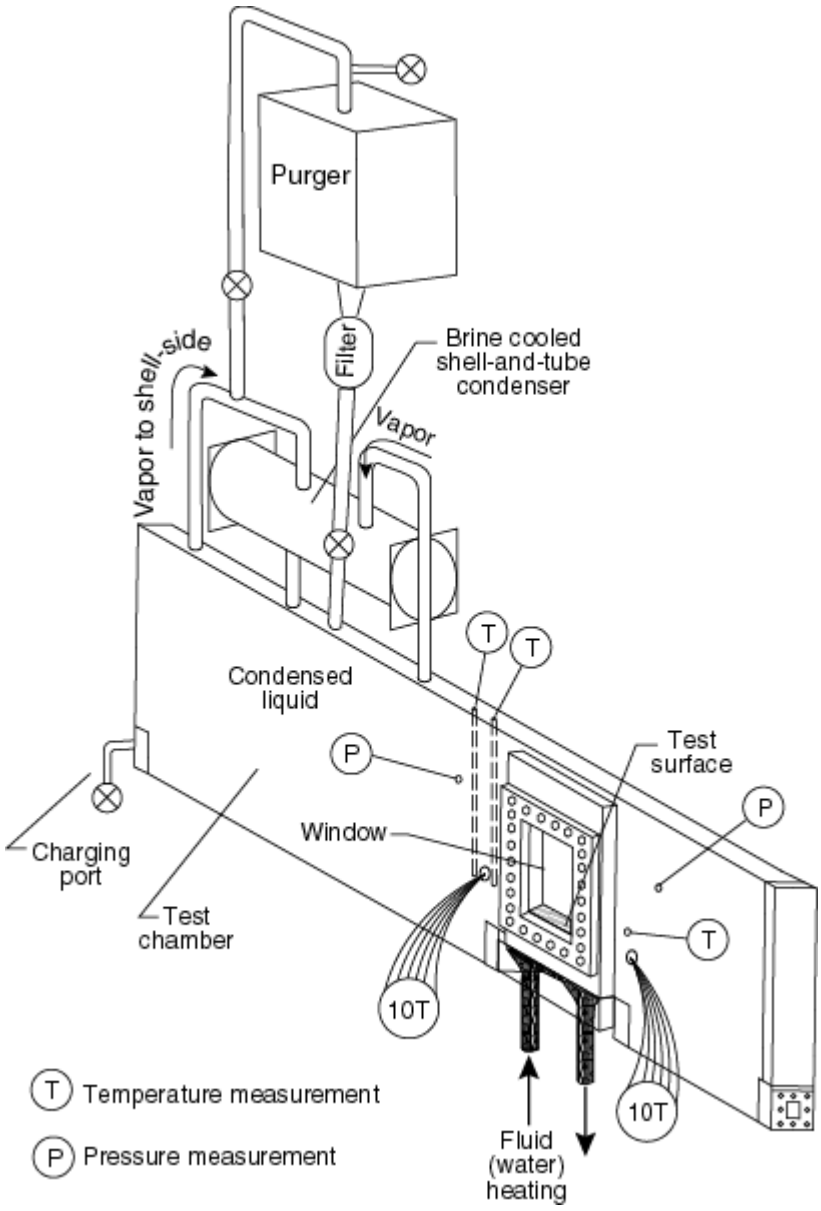

Fig. 1 Schematic of test apparatus

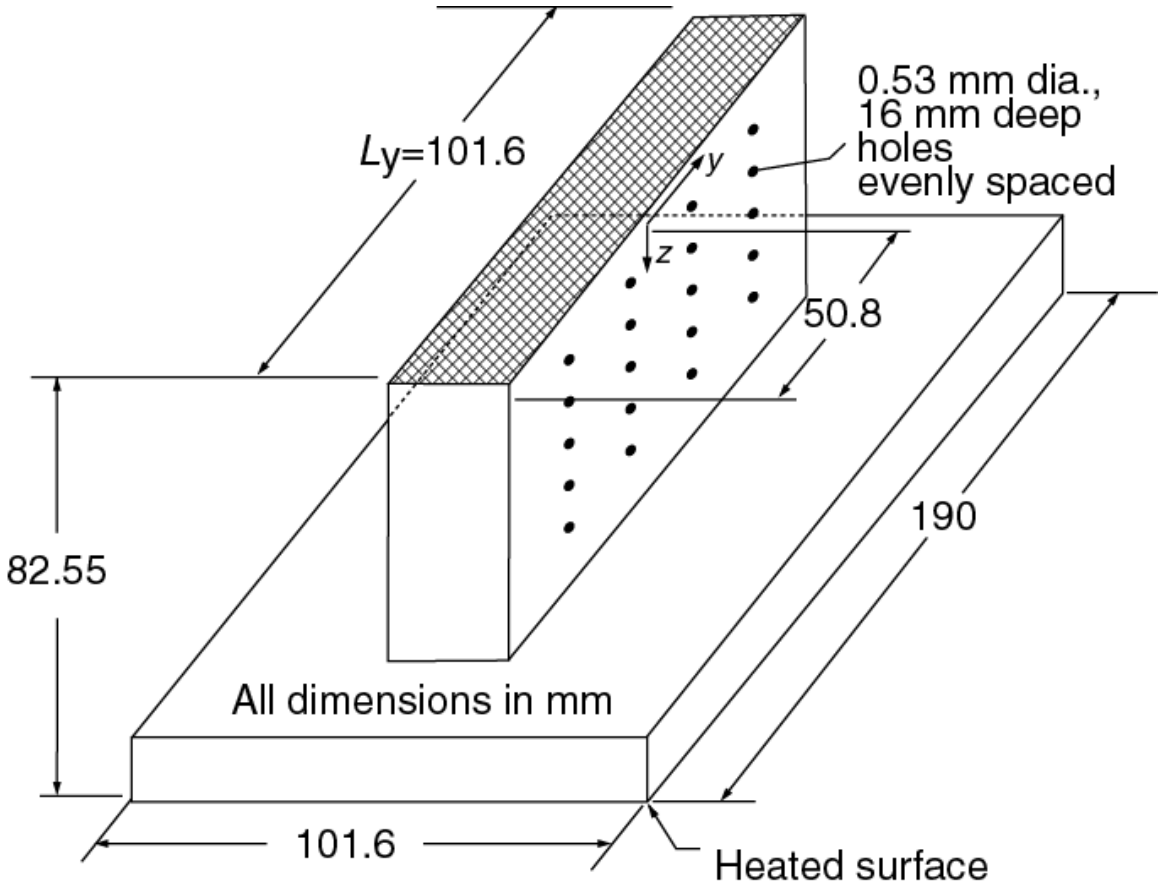

Fig. 2 OFHC copper flat test plate with cross-hatched surface and thermocouple coordinate system

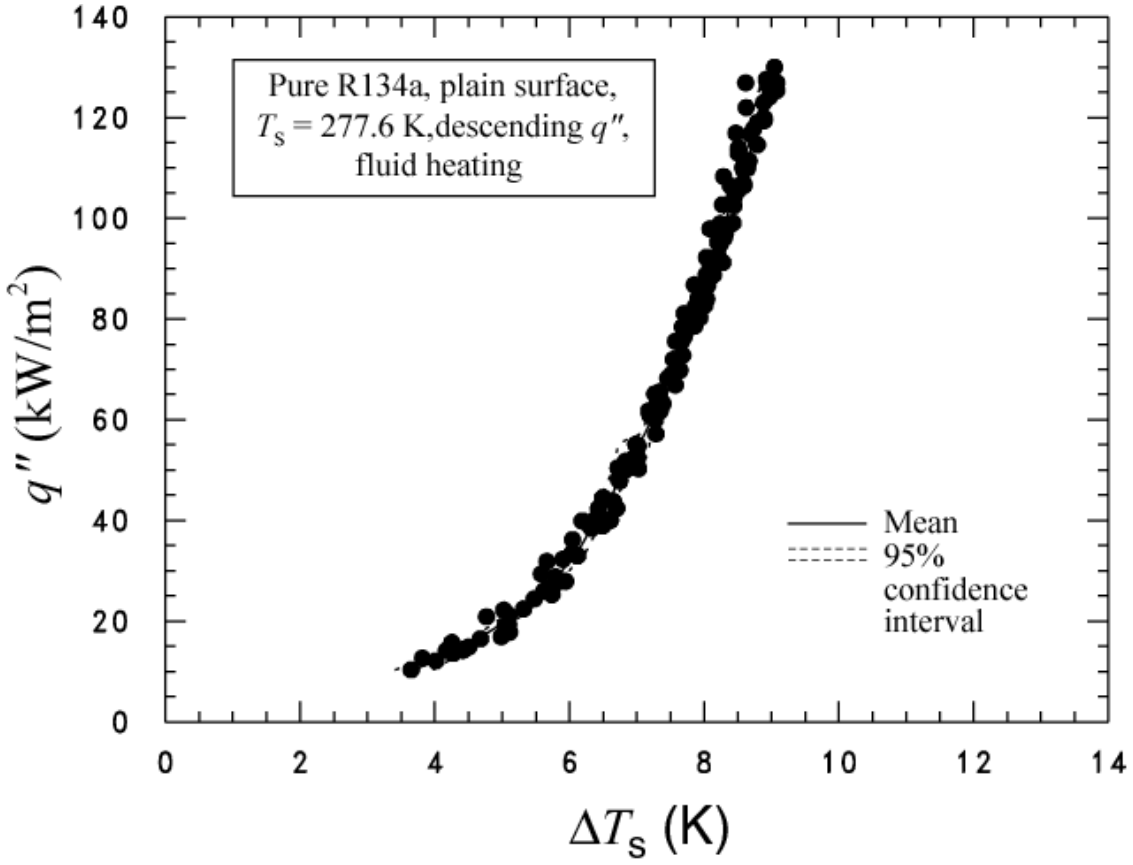

Fig. 3 Pure R134a boiling curve for plain surface

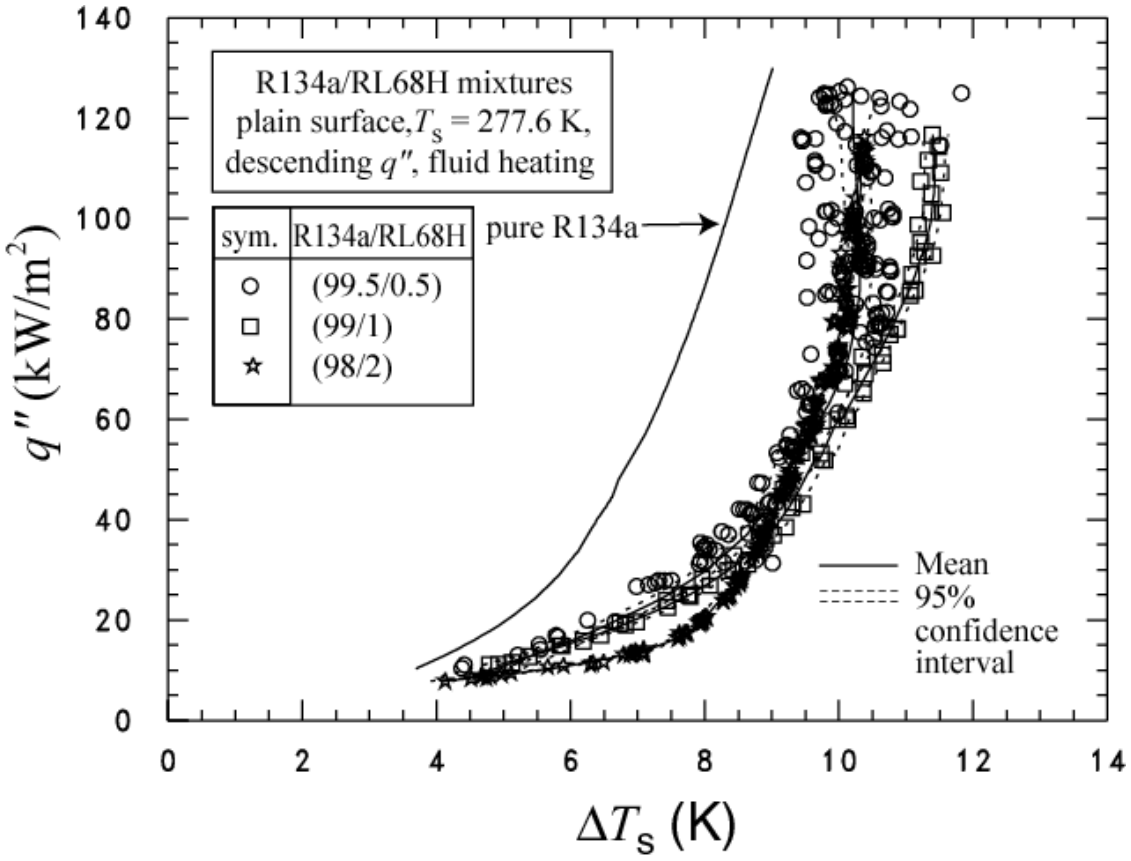

Fig. 4 R134a/RL68H mixtures boiling curves for plain surface

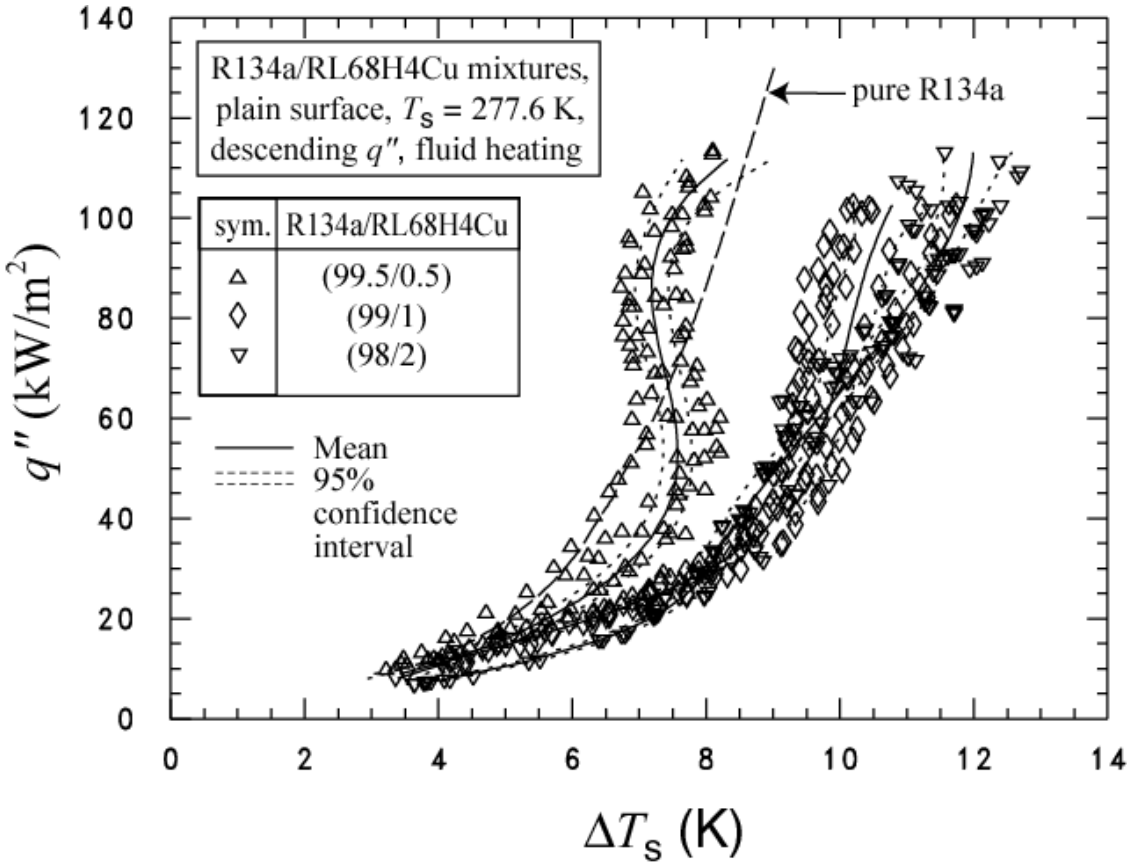

Fig. 5 R134a/RL68H with 4 % volume CuO mixtures boiling curves for plain surface

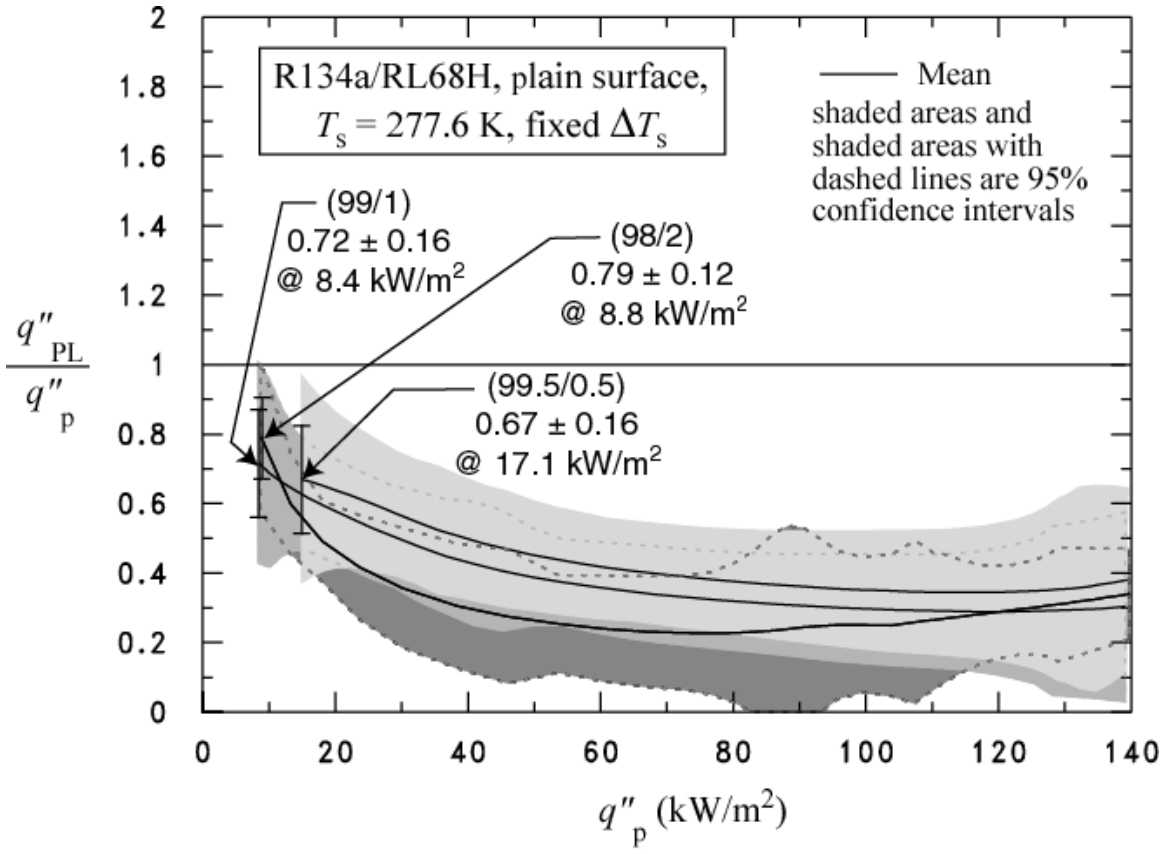

Fig. 6 R134a/RL68H mixture heat flux relative to that of pure R134a for a plain surface

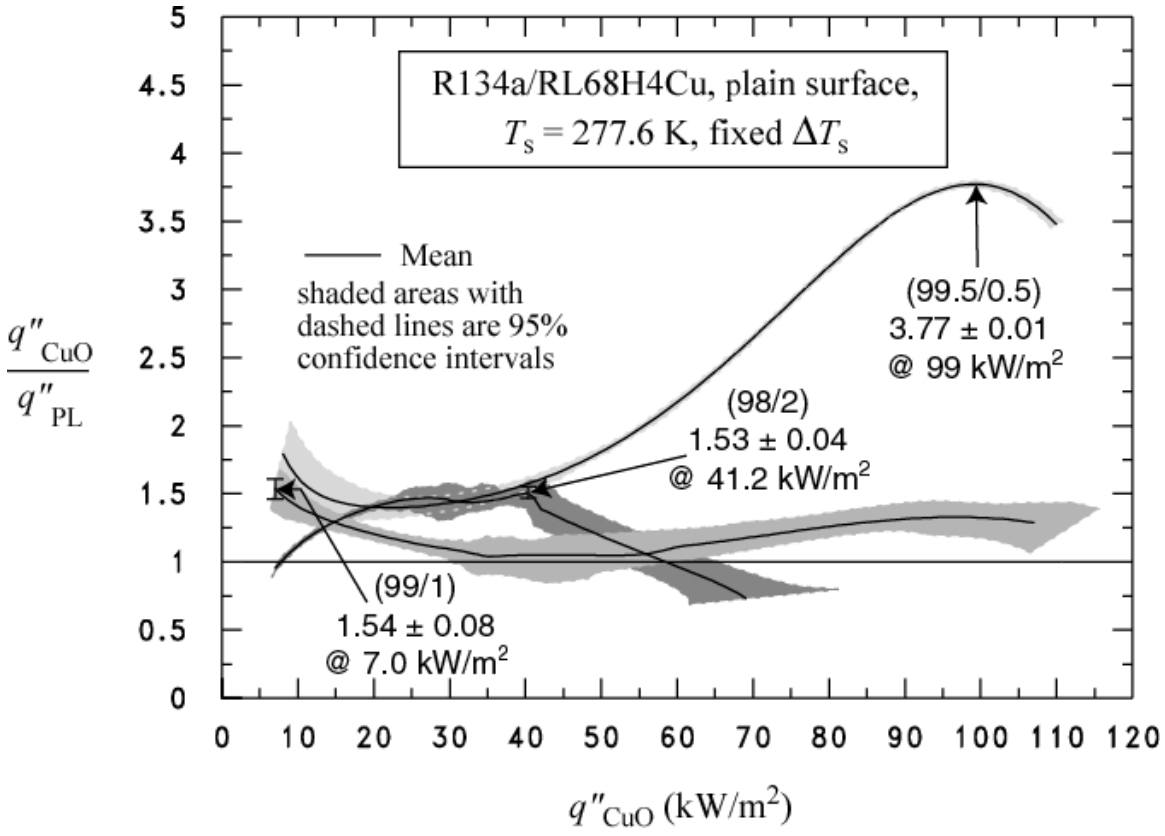

Fig. 7 Boiling heat flux of R134a/RL68H4Cu mixtures relative to that of pure R134a for a plain surface

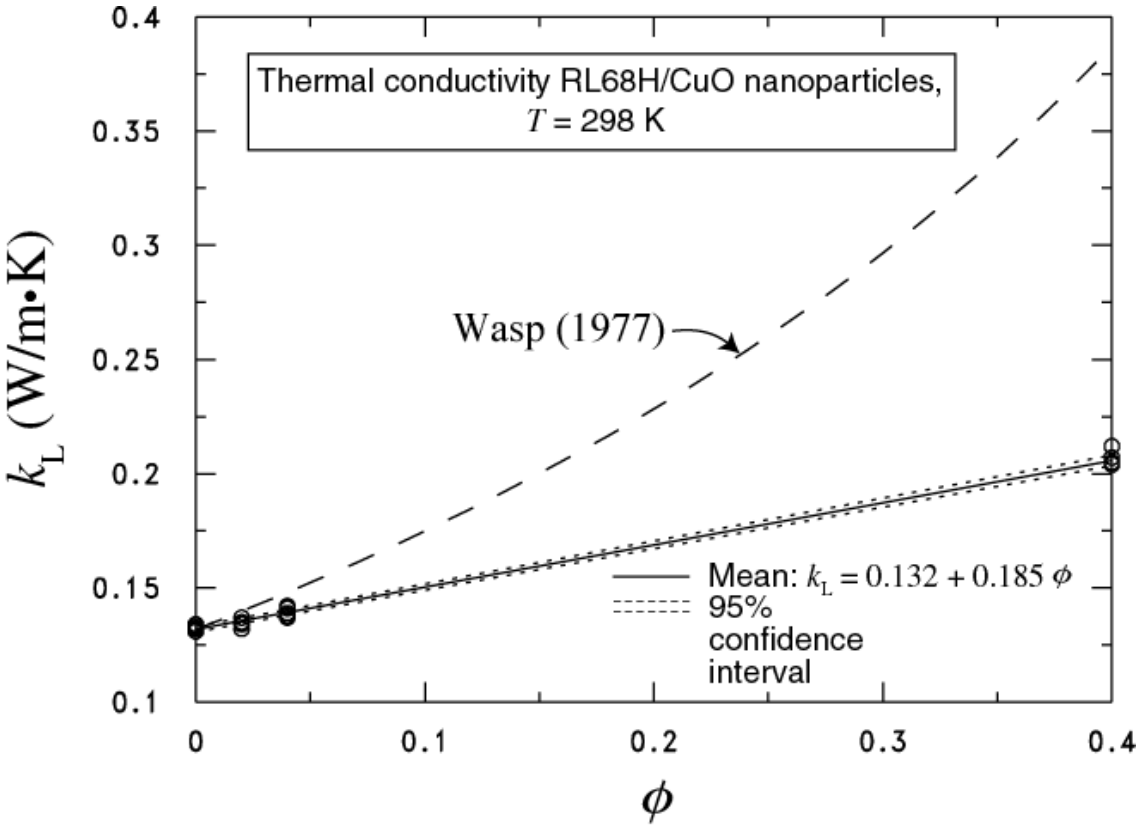

Fig. 8 Measured thermal conductivity of RL68H/CuO nanoparticles mixtures as a function of volume fraction of CuO

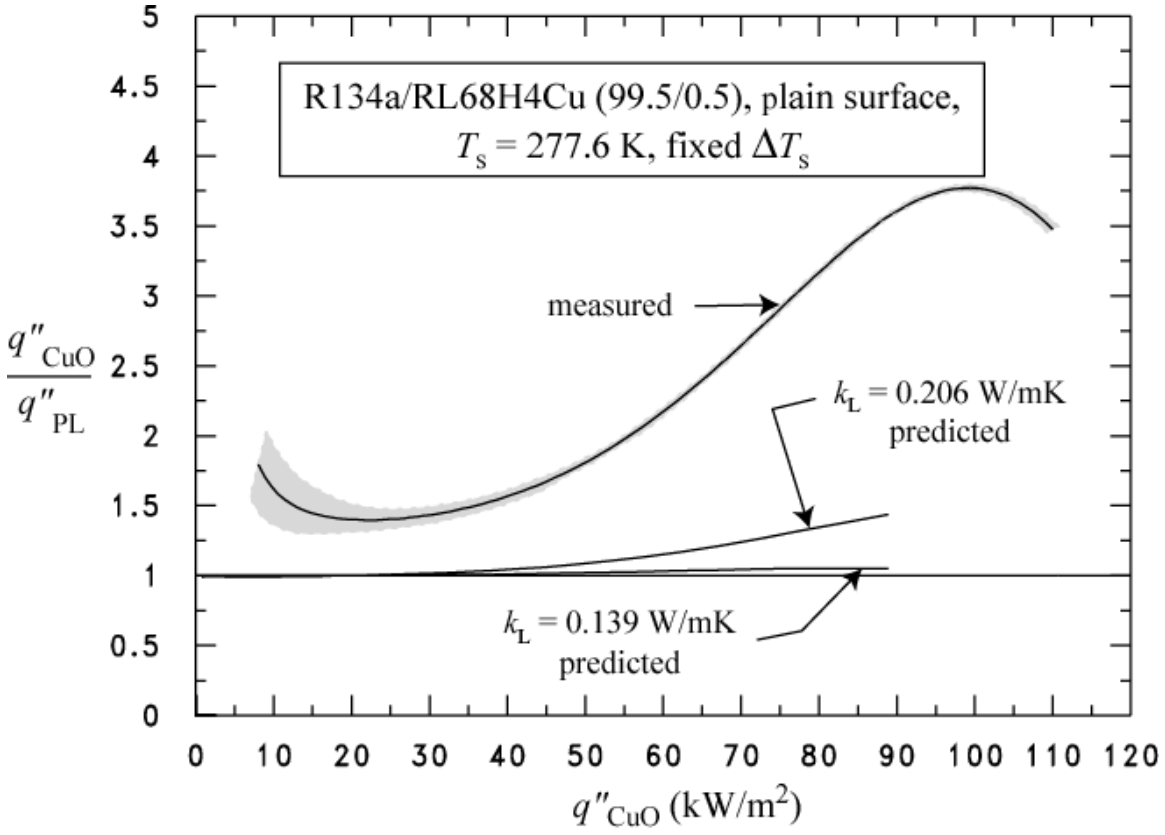

Fig. 9 Predicted heat flux ratio for RL68H4Cu (99.5/0.5) mixture using Kedzierski (2003b) model

APPENDIX A: UNCERTAINTIES

Figure A.1 shows the relative (percent) uncertainty of the heat flux ($U_{q''}$) as a function of the heat flux. Figure A.2 shows the uncertainty of the wall temperature as a function of heat flux. The uncertainties shown in Figs. A.1 and A.2 are "within-run uncertainties." These do not include the uncertainties due to "between-run effects" or differences observed between tests taken on different days. The "within-run uncertainties" include only the random effects and uncertainties associated with one particular test. All other uncertainties reported in this study are "between-run uncertainties" which include all random effects such as surface past history or seeding.

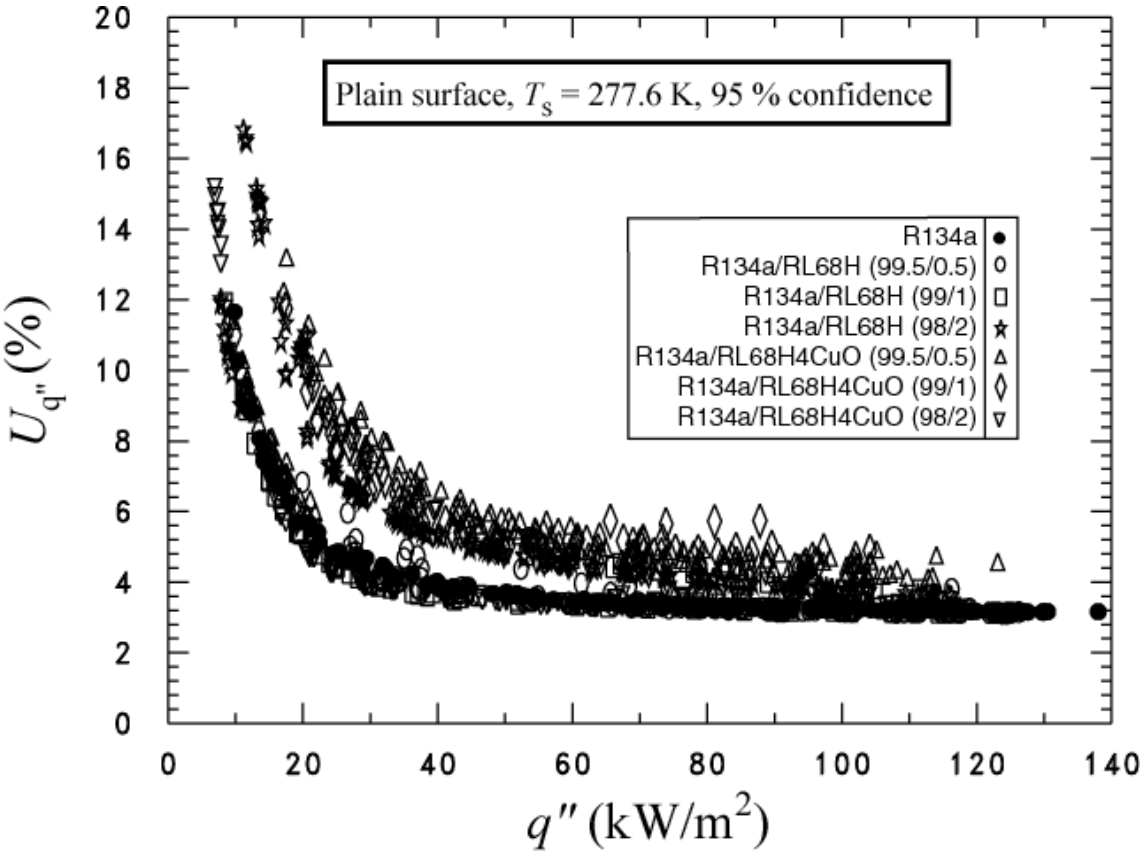

Fig. A.1 Expanded relative uncertainty in the heat flux of the surface at the 95 % confidence level

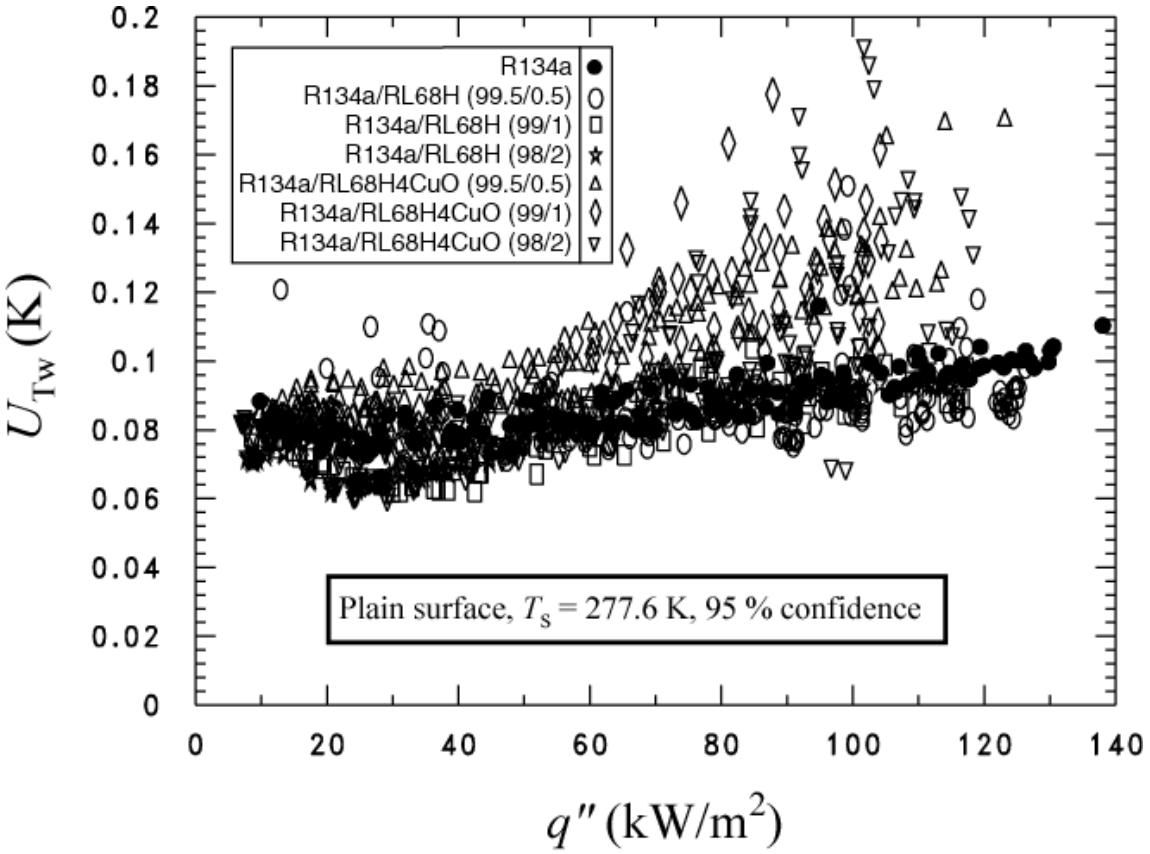

Fig. A.2 Expanded uncertainty in the temperature of the surface at the 95 % confidence level

APPENDIX B: LUBRICANT LIQUID DENSITY MEASUREMENTS

This appendix presents the measurements and the correlation of the RL68H, and the RL68H with 40 % volume CuO nanoparticles liquid densities (ρ). The density of the liquid lubricant was measured as a function of temperature with a glass pycnometer. The pycnometer was factory instrumented with a glass mercury thermometer with a range of 14 °C to 38 °C in 0.2 °C graduations, accurate to within ± 0.2 °C. The pycnometer was filled with distilled water and its volume was calculated from the known density of water. The volume was found with 29 trials to be 9.588 ml with a standard uncertainty of 0.002 ml. The average mass of the pycnometer after nine trials was 28.794 g ± 0.001 g.

The pycnometer containing the RL68H lubricant was cooled in an ice bath and then removed from the bath and allowed to warm on the balance to room temperature over approximately one hour. The standard uncertainty of the balance was approximately 1 mg. The outside of the pycnometer was wiped clean before each measurement to remove the lubricant that was expelled through the pipette due to volume expansion with temperature increase.

The Biot number for the warming pycnometer was estimated to be approximately 0.5, which is greater than the recommended limit of 0.1 (Incropera and Dewitt, 1985) for a uniform temperature in fluid. It is difficult to estimate the error introduced in the measurements due to temperature gradients that existed in the lubricant. However, the data regression shows that the residuals are independent of temperature, which suggests that the error due to temperature gradients in the liquid had a negligible effect on the density measurements.

Tables B.1 shows the recorded measurements for the RL68H lubricant. Equation B.1 gives the fit of the liquid lubricant density (ρ_l) in kg/m^3 versus temperature (T) in Kelvin:

$$\rho_l = 1146 - 0.6336T \qquad \text{B.1}$$

The expanded uncertainty of the fits were approximately ± 1 kg/m^3 for 95 % confidence.

The density of the RL68H with 40 % volume CuO nanoparticles (ρ_L) was measured at a single temperature (297.6 K) and found to be 1447.9 kg/m^3 ± 0. 3 kg/m^3.

The density of the CuO particles at 297.6 K (ρ_{np}) can be obtained from the mixture combination rule (Reid et al., 1977) between density and volume fraction for the 40 % volume nanolubricant solution:

$$\rho_L = 0.4\rho_{np} + (1-0.4)\rho_l \qquad \text{B.2}$$

Solving eq (B.2) for the density of the nanoparticles yields 2183.4 kg/m^3. The same form of eq (B.2) is obtained when the mass-fraction-based mixture density equation for suspensions given by Wasp (1977) is re-written interms of volume fraction.

Table B.1 RL68H liquid density measurements

T (°C)	Lubricant mass (g)	ρ_l (kg/m^3)
16	9.241	963.80
17	9.234	963.07
17.8	9.228	962.44
18.4	9.223	961.92
19.2	9.217	961.29
20	9.212	960.77
20.6	9.207	960.25
21.2	9.201	959.62
22.2	9.197	959.21
22.8	9.191	958.58
23.8	9.184	957.85
24.2	9.182	957.64
14.2	9.235	963.17
15.4	9.229	962.54
17.8	9.222	961.82
18.6	9.214	960.98
19.4	9.21	960.56
20	9.207	960.25
21.2	9.2	959.52
21.8	9.197	959.21
22.8	9.19	958.48
23.4	9.184	957.85
24.2	9.181	957.54
14.4	9.236	963.28
15.8	9.226	962.23
17.2	9.221	961.71
18.4	9.211	960.69
19.4	9.206	960.15
20.6	9.201	959.62
21.6	9.195	959.00
22.6	9.189	958.37
23.4	9.182	957.64
24	9.175	956.91

APPENDIX C: DILUTION OF 40 % VOLUME NANOLUBICANT

This appendix presents the analysis that was used to dilute the 40 % copper (II) oxide volume fraction nanolubricant to a 4 % copper (II) oxide volume fraction. The uncertainty of the target (diluted) volume fraction is also discussed.

The volume fraction of the initial mixture (ϕ_i) is expressed in terms of the volume of the CuO particles (V_{np}) and the volume of the initial neat lubricant (V_{li}):

$$\phi_i = \frac{V_{np}}{V_{np} + V_{li}} \tag{C.1}$$

Likewise, the desired volume fraction of the target mixture (ϕ_t) is obtained by diluting the initial mixture with an additional volume of neat lubricant (V_{l+}):

$$\phi_t = \frac{V_{np}}{V_{np} + V_{li} + V_{l+}} \tag{C.2}$$

Equations C.1 and C.2 can be simultaneously solved for the additional volume of neat lubricant required to dilute ϕ_i to ϕ_t:

$$V_{l+} = V_{li} \frac{\phi_i - \phi_t}{\phi_t - \phi_t \phi_i} \tag{C.3}$$

Equation C.3 can be written in terms of the density of the initial nanolubricant mixture (ρ_L)[7] and the mass of the initial nanolubricant sample to be diluted (M_{Ti}):

$$V_{l+} = \frac{M_{Ti}}{\rho_L\big|_{\phi_i}} \left(\frac{\phi_i}{\phi_t} - 1 \right) \tag{C.4}$$

Equation C.4 can be written in terms of the mass of neat lubricant to be added to obtain the target dilution (M_{l+}) with use of the neat lubricant density (ρ_l):

$$M_{l+} = V_{l+} \rho_l = \frac{M_{Ti} \rho_l}{\rho_L\big|_{\phi_i}} \left(\frac{\phi_i}{\phi_t} - 1 \right) \tag{C.5}$$

[7] The ρ_m measurement was presented in Appendix B.

The total mass of the target mixture (M_{Tt}) is the sum of M_{Ti} and $M_{\mathrm{l+}}$. This mass balance and eq (C.5) can be used to calculate the required $M_{\mathrm{l+}}$ as:

$$M_{\mathrm{l+}} = \frac{M_{\mathrm{Tt}}}{1+\left(\frac{\phi_{\mathrm{t}}}{\phi_{\mathrm{i}}-\phi_{\mathrm{t}}}\right)\frac{\rho_{\mathrm{L}}\big|_{\phi_{\mathrm{i}}}}{\rho_{\mathrm{l}}}} \tag{C.6}$$

The volume fraction of the target mixture is expressed as:

$$\phi_{\mathrm{t}} = \frac{\phi_{\mathrm{i}} M_{\mathrm{Ti}}}{M_{\mathrm{Ti}} + \frac{\rho_{\mathrm{L}}\big|_{\phi_{\mathrm{i}}}}{\rho_{\mathrm{l}}} M_{\mathrm{l+}}} \tag{C.5}$$

where the dominant uncertainty of ϕ_{t} is the uncertainty of ϕ_{i}. All of the other eq (C.5) parameters combined cause only a 0.1 % uncertainty in ϕ_{t} for the dilution of the 40 % volume fraction solution to a 4 % volume fraction. The uncertainty in ϕ_{i} is a b-type uncertainty because it comes from the manufacturer as ± 1 %. Consequently, the total uncertainty in ϕ_{t} is approximately ± 1 %.

APPENDIX D: CAPILLARY RISE MEASUREMENTS

This appendix presents capillary rise measurements for RL68H at approximately 25 ºC. Table D.1 provides the capillary rise height measurements (l) that were used to calculate the surface tension for the lubricant. The standard deviation of the mean measurement for this method was approximately 0.5 % of the measurement.

A force balance on the column of liquid in the capillary tube was used to calculate the surface tension (Adamson and Gast, 1997):

$$\sigma = \frac{r\Delta\rho g l}{2} \approx \frac{r\rho_l g l}{2} \tag{D.1}$$

where the measured radius of the capillary tube (r) was 0.97 mm with a B-type estimated uncertainty of ± 0.03 mm. The liquid density (ρ_l) measurement is given in Appendix B. The uncertainty of the density measurements is approximately ± 1 kg/m^3.

The liquid-vapor (air) surface tensions as calculated from eq (D.1) for the RL68H was 0.0277 N/m ± 0.0006 N/m at 297.97 K.

Table D.1 Capillary rise measurements for RL68H

T (ºC)	l (mm)	ρ (kg·m^{-3})	σ (N·m^{-1})
24.813	23	957.18	0.0281
24.815	22.5	957.18	0.0275
24.816	22.5	957.18	0.0275
24.817	22.5	957.18	0.0275
24.817	22.5	957.18	0.0275
24.818	22.5	957.18	0.0275
24.818	22.5	957.18	0.0275
24.819	23	957.17	0.0281
24.819	23	957.17	0.0281
24.82	23	957.17	0.0281
24.82	22.5	957.17	0.0275
24.82	22.5	957.17	0.0275
24.82	22.5	957.17	0.0275

APPENDIX E: LUBRICANT VISCOSITY MEASUREMENTS

This appendix presents the liquid kinematic viscosity measurements for RL58H at approximately 25 ºC in Table E.1. A glass viscometers at the appropriate viscosity range was used to measure the liquid viscosities of the lubricant. The B-type uncertainty of the viscometer was quoted by the manufacturer as 0.22 % of the measurement. The average measured viscosity of the lubricant, for the 95 % confidence level, was 85 $\mu m^2/s \pm 1.5$ $\mu m^2/s$.

A model 300 viscometer with a viscosity range of 50 $\mu m^2/s$ to 250 $\mu m^2/s$ was used. The calibration constant (C_o) for the viscosity was a function of viscometer/liquid temperature:

$$C_o = 0.24317 - 1.6667 \times 10^{-5} T \qquad \text{(D.1)}$$

where T is in Celsius and C_o is in $\mu m^2/s$.

The kinematic viscosity in $\mu m^2/s$ was obtained by multiplying the measured efflux time in seconds by C_o. The averaged measured viscosity of RL68H at an average temperature of 297.74 K was 144 $\mu m^2/s \pm 1.9$ $\mu m^2/s$.

Table E.1 Kinematic viscosity measurements for RL68H

T (ºC)	Efflux time (s)	C_o ($\mu m^2/s$)	ν ($\mu m^2/s$)
24.576	583.12	0.242757067	141.56
24.583	606.02	0.24275695	147.12
24.59	606.44	0.242756833	147.22
24.598	606.9	0.2427567	147.33
24.603	606.77	0.242756617	147.30
24.61	608.6	0.2427565	147.74